Late Pleistocene climate change and landscape dynamics in the Eastern Alps: the inner-alpine Unterangerberg record (Austria)

Starnberger, R., Drescher-Schneider, R., Reitner, J. M., Rodnight, H., Reimer, P. J., & Spoetl, C. (2013). Late Pleistocene climate change and landscape dynamics in the Eastern Alps: the inner-alpine Unterangerberg record (Austria). Quaternary Science Reviews, 68, 17-42. DOI: 10.1016/j.quascirev.2013.02.008

Published in:
Quaternary Science Reviews

Document Version:
Publisher's PDF, also known as Version of record

Quaternary Science Reviews 68 (2013) 17–42

Contents lists available at SciVerse ScienceDirect

Quaternary Science Reviews

journal homepage: www.elsevier.com/locate/quascirev

Late Pleistocene climate change and landscape dynamics in the Eastern Alps: the inner-alpine Unterangerberg record (Austria)

Reinhard Starnberger [a,*], Ruth Drescher-Schneider [b], Jürgen M. Reitner [c], Helena Rodnight [a], Paula J. Reimer [d], Christoph Spötl [a]

[a] Institute for Geology and Palaeontology, Leopold-Franzens University of Innsbruck, Innrain 52, 6020 Innsbruck, Austria
[b] Institute of Plant Sciences, Karl-Franzens University of Graz, Holteigasse 6, 8010 Graz, Austria
[c] Geological Survey of Austria, Neulinggasse 38, 1030 Vienna, Austria
[d] Centre for Climate, the Environment & Chronology (14CHRONO), School of Geography, Archaeology and Palaeoecology, Queen's University Belfast, Belfast BT7 1NN, UK

ARTICLE INFO

Article history:
Received 2 October 2012
Received in revised form
4 February 2013
Accepted 7 February 2013
Available online 16 March 2013

Keywords:
Late Pleistocene
Lake sediments
European Alps
Luminescence dating
Pollen analysis
Stratigraphy

ABSTRACT

Drill cores from the inner-alpine valley terrace of Unterangerberg, located in the Eastern Alps of Austria, offer first insights into a Pleistocene sedimentary record that was not accessible so far. The succession comprises diamict, gravel, sand, lignite and thick, fine grained sediments. Additionally, cataclastic deposits originating from two paleo-landslide events are present. Multi-proxy analyses including sedimentological and palynological investigations as well as radiocarbon and luminescence data record the onset of the last glacial period (Würmian) at Unterangerberg at ~120–110 ka. This first time period, correlated to the MIS 5d, was characterised by strong fluvial aggradation under cold climatic conditions, with only sparse vegetation cover. Furthermore, two large and quasi-synchronous landslide events occurred during this time interval. No record of the first Early Würmian interstadial (MIS 5c) is preserved. During the second Early Würmian interstadial (MIS 5a), the local vegetation was characterised by a boreal forest dominated by Picea, with few thermophilous elements. The subsequent collapse of the vegetation is recorded by sediments dated to ~70–60 ka (i.e. MIS 4), with very low pollen concentrations and the potential presence of permafrost. Climatic conditions improved again between ~55 and 45 ka (MIS 3) and cold-adapted trees re-appeared during interstadials, forming an open forest vegetation. MIS 3 stadials were shorter and less severe than the MIS 4 at Unterangerberg, and vegetation during these cold phases was mainly composed of shrubs, herbs and grasses, similar to what is known from today's alpine timberline. The Unterangerberg record ended at ~45 ka and/or was truncated by ice during the Last Glacial Maximum.

1. Introduction

Tracking Late Pleistocene climatic changes and their impact on the environment and landscape evolution is a challenging task for Quaternary science, aimed at a better understanding of the underlying forcing and internal feedback processes. In this context, mountain ranges are of particular interest as they are highly sensitive to climate change such as the current warming trend (Beniston, 2003; Huber et al., 2005).

The European Alps are one of the best studied mountain ranges in the world. Here, the regional impact of global climatic changes, expressed e.g. by fluctuations of the equilibrium line altitude, the tree line and lake levels, is well documented for the Late Glacial and the Holocene (e.g., Nicolussi et al., 2005; Magny, 2007; Joerin et al., 2008). However, the Last Glacial Maximum (LGM), the most dramatic interval of the Late Pleistocene, eradicated most of the older sedimentary archives, especially inside of the Alps. Hence, paleodata for the pre-LGM are much less abundant than for the Late Glacial and Holocene, and records are often truncated and difficult to date. For up-to-date reviews of the Late Pleistocene history of the Alps the reader is referred to van Husen (2004), Preusser (2004), Schlüchter (2004), and Ivy-Ochs et al. (2008).

The start of the last glacial period in the Alps (Würm *sensu* Chaline and Jerz, 1984) is best recorded by a steep decline in oxygen isotope values of speleothems around 118 ka, indicating major atmospheric cooling (Spötl et al., 2007; Meyer et al., 2008). The glacial inception thus occurred within dating uncertainties of the transition from the Eemian into the first cold phase in Greenland,

* Corresponding author.
E-mail address: reinhard.starnberger@uibk.ac.at (R. Starnberger).

0277-3791
http://dx.doi.org/10.1016/j.quascirev.2013.02.008

i.e. Greenland Stadial 26 (NGRIP project members, 2004). Whether this first Early Würmian stadial) resulted in a large advance of alpine glaciers is still a matter of debate (Ivy-Ochs et al., 2008). While there are data suggesting such a major advance in the Western Alps (Preusser et al., 2003; Preusser et al., 2007), observations from the Eastern Alps show that the main valleys remained ice-free during this time (Reitner, 2005; Spötl and Mangini, 2006). The Early Würmian was characterised by two prominent interstadials (corresponding to MIS 5c and 5a) with conifer forests and timber lines 100–300 m lower than today (Drescher-Schneider, 2000). The timing of a third, forested interstadial (Dürnten) is still controversial (see e.g. Preusser, 2004; Ivy-Ochs et al., 2008). The equivalent of MIS 4 is poorly recorded in sedimentary successions around the Alps. Data from the Western Alps (e.g. Welten, 1982; Schlüchter, 1991; Preusser et al., 2003) again suggest a major ice advance, while no such evidence has been found so far in the Eastern Alps. Data from speleothems complement this latter picture and show a high degree of $\delta^{18}O$ synchronicity between the Alps and the North Atlantic region during MIS 5 to 4 (Boch et al., 2011). The Middle Würmian (sensu Chaline and Jerz, 1984) largely corresponds to MIS 3 and the period of the most pronounced Dansgaard–Oeschger (DO) climatic events as known e.g. from Greenland (Dansgaard et al., 1993). These rapid climate changes are only rarely recorded by sediments in the Alps and the northern alpine foreland (e.g., by speleothems, lake and loess deposits; Haesaerts et al., 1996; Spötl et al., 2006; Anselmetti et al., 2010; Thiel et al., 2011; Dehnert et al., 2012) and suggest a long-term climatic deterioration towards the end of MIS 3 leading eventually to maximum ice extent during the LGM (MIS 2).

In short, aeolian and fine-grain waterlain sediments, in conjunction with cave deposits, permit the tracing of the general outline of the climate evolution in the Alps during the Upper Pleistocene and underscore the correspondence with the North Atlantic climate. Major unknowns include the magnitude and timing of pre-LGM ice advances and the response of the alpine environment to D-O events and their impact on the ecosystem. The present study aims to fill part of this significant gap by providing an inner-alpine perspective of climatic and environmental change prior to the LGM from a newly studied and – thanks to a series of fully cored drill holes – exceptionally well-characterized site in the Austrian Alps. We employ a multi-proxy approach and use several dating techniques to advance the understanding of Late Pleistocene climate variability and its impact on the regional scale. This study also provides new data on pre-LGM landslides which are currently amongst the oldest dated mass movements in the Alps.

2. Regional setting

The Inn valley is one of the largest valleys in the Alps, characterised by overdeepening due to repeated Pleistocene glaciations, e.g. at Kramsach, (40 km northeast of Innsbruck), where a drill hole reached the base of the Quaternary sediment fill 180 m below today's valley floor level (Preusser et al., 2010). Surrounded by mountains with altitudes of up to 2500 m a.s.l., valley terraces are a characteristic element of this landscape. Our study site, the terrace of Unterangerberg, is located northwest of the city of Wörgl (Fig. 1). The surface of this terrace lies approximately 150 m above the valley floor, covering an area of ~34 km^2 and bounded by the river Inn in the southeast.

Field evidence shows that the basis of the terrace is formed by partly lithified fluvial sediments of the Upper Oligocene Angerberg Formation (e.g. Ampferer, 1922; Ortner and Stingl, 2001). These are overlain by Pleistocene sediments first described by Penck and Brückner (1909), and later by Ampferer and Ohnesorge (1909), von Klebelsberg (1935) and Heissel (1951, 1955). LGM-lodgement till tops the sequence. Additionally, cataclasite deposits originating from two individual landslide events are embedded in the Pleistocene sediments. Although already described by Penck and Brückner (1909), only one of these events has been investigated in greater detail so far (Gruber et al., 2009).

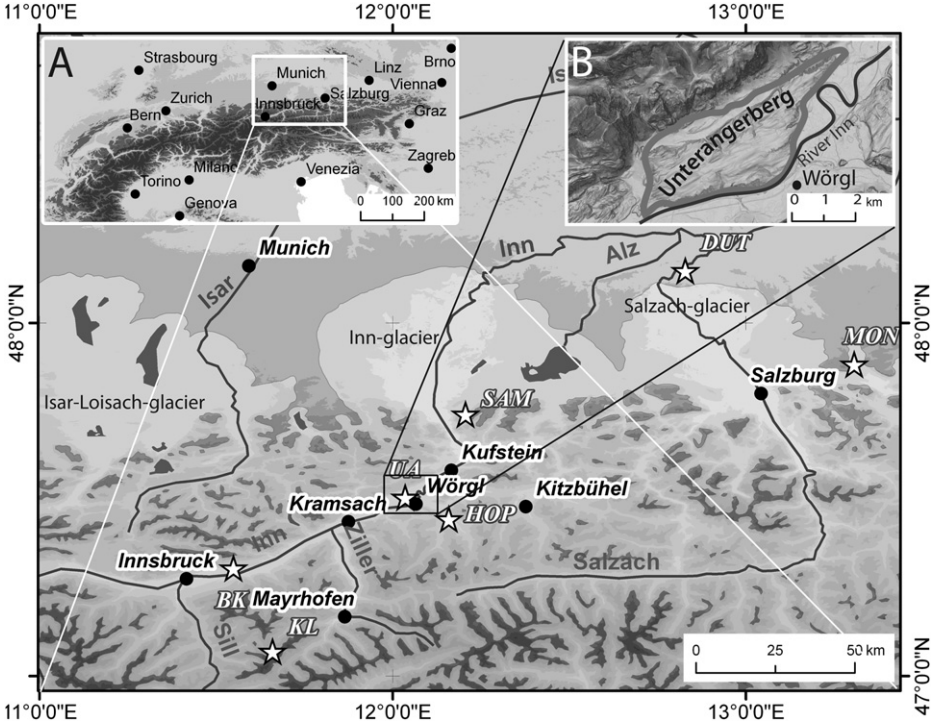

Fig. 1. Regional setting of the Unterangerberg terrace (inset B) in the northern Alps (inset A) and their foreland; asterisks mark the Unterangerberg site (UA) as well as important other key sites: KL = Kleegruben Cave; BK = Baumkirchen; HOP = Hopfgarten basin; SAM = Samerberg; MON = Mondsee.

Between 1995 and 2006, geophysical investigations and numerous drillings were performed on the Unterangerberg terrace under the supervision of the Brenner–Eisenbahn–Gesellschaft (BEG) as part of a tunnel prospection campaign. These resulted in a model of the bedrock topography in the subsurface of the terrace (Fig. 2). Here, the main feature is a SW-NE striking depression filled by up to 150 m of Pleistocene sediments. This depression is bounded in the south and southeast by a series of small swells.

3. Materials and methods

3.1. Lithological description and lithofacies types

This study is based on the exclusive access to cores recovered from the Unterangerberg terrace during drilling campaigns in 1998 and 2006 which provided unprecedented insights into this otherwise poorly exposed terrain. In total, 17 cores with lengths between ~40 m and 200 m were available, offering insights into the Oligo- and Pleistocene sediments filling of the terrace (Fig. 3). Description of the cores was made based on the criteria described in Table 1. However, this was hampered by the fact that drilling disturbed parts of the cores, especially those containing coarse-grained and poorly consolidated sediment. Sediment units were defined and lithofacies codes were designated following Keller (1996), Benn and Evans (1998), Krüger and Kjær (1999) and Tucker (2003). This led to the genetic interpretation of different sediment facies types (Table 1). Grain size analysis was performed using wet sieving for coarse-grained, and laser diffraction using a Malvern Instruments Mastersizer 2000 (Sperazza et al., 2004) for fine-grained samples.

3.2. Pollen analysis

For pollen analysis, sediment samples of ~300 g each were taken from the cores. Based on the lithological description, a first sampling campaign concentrated on the organic-rich core sections A-KB 15/98 (16–20 m), A-KB 16/98 (30–46 m) and A-KB 17/98 (26–46 m depth), with sampling increments of 20 cm for most parts. As a next step, sampling was extended to other organic-bearing sequences identified in A-KB 14/98 (43.5–50.2) m and A-KB 15/98 (~52.5 m) depth. In order to investigate also core sections for which expectations were low due to the lithological account, test samples from A-KB 13/98 (31–51.5 m), A-KB 14/98 (62–82 m) and A-KB 15/98 (79–143 m) were taken.

A total of 184 samples from cores A-KB 13/98, A-KB 14/98, A-KB 15/98, A-KB 16/98 and A-KB 17/98 was chemically treated using HCl, HF, and acetolysis. Following Stockmarr (1971), marker spores (*Lycopodium*) were added to 1–2 ml of sediment to allow the calculation of pollen concentration. Of these, 140 samples were palynologically investigated. Pollen concentrations ranged from zero in some massive fine-grain (Fm) sections to ~40,000 grains/ml in organic-rich fine-grain samples and ~270,000 grains/ml in fine detrital gyttja samples. For statistically significant vegetation reconstructions at least 500 pollen grains per sample should be counted (Berglund and Ralska-Jasiewiczowa, 1986). In samples with low pollen concentrations an entire slide (24 × 32 mm) was analysed. For the determination of pollen types, the pollen key of Beug (2004) and the private reference collections of R. Drescher-Schneider were used. The identification of the non-pollen palynomorphs (NPP) is based on Van Geel (1978) and Van Geel et al. (1981, 1983, 1989). The determination of the Neorhabdocoela follows the description by Haas (1995). For calculation of percentages, Cyperaceae, Pteridophytes, aquatics, pre-Quaternary sporomorphs, and indeterminanda are excluded from the pollen sum (arboreal (AP) and non arboreal pollen (NAP) = 100%). The percentages of Cyperaceae refer to the pollen sum including Cyperaceae. The spores of ferns and mosses and the NPPs (includes algae, fungi, mandibles of chironomids, and other remains of invertebrates) are expressed referring to the pollen sum. The results are presented as reduced percentage pollen diagrams (for the complete data set see Appendix A). Local pollen zones (LPZ) are defined manually

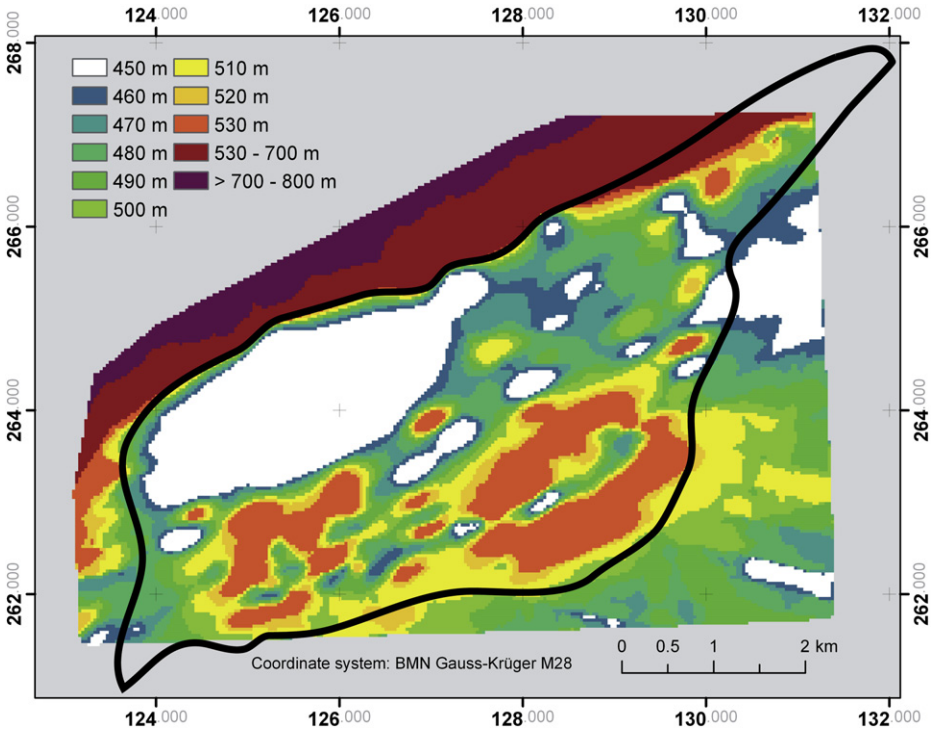

Fig. 2. Bedrock topography of the Unterangerberg terrace (solid line) underneath the Pleistocene sediment fill as derived from geophysical data. Elevations are given relative to sea level (Poscher et al., 2008).

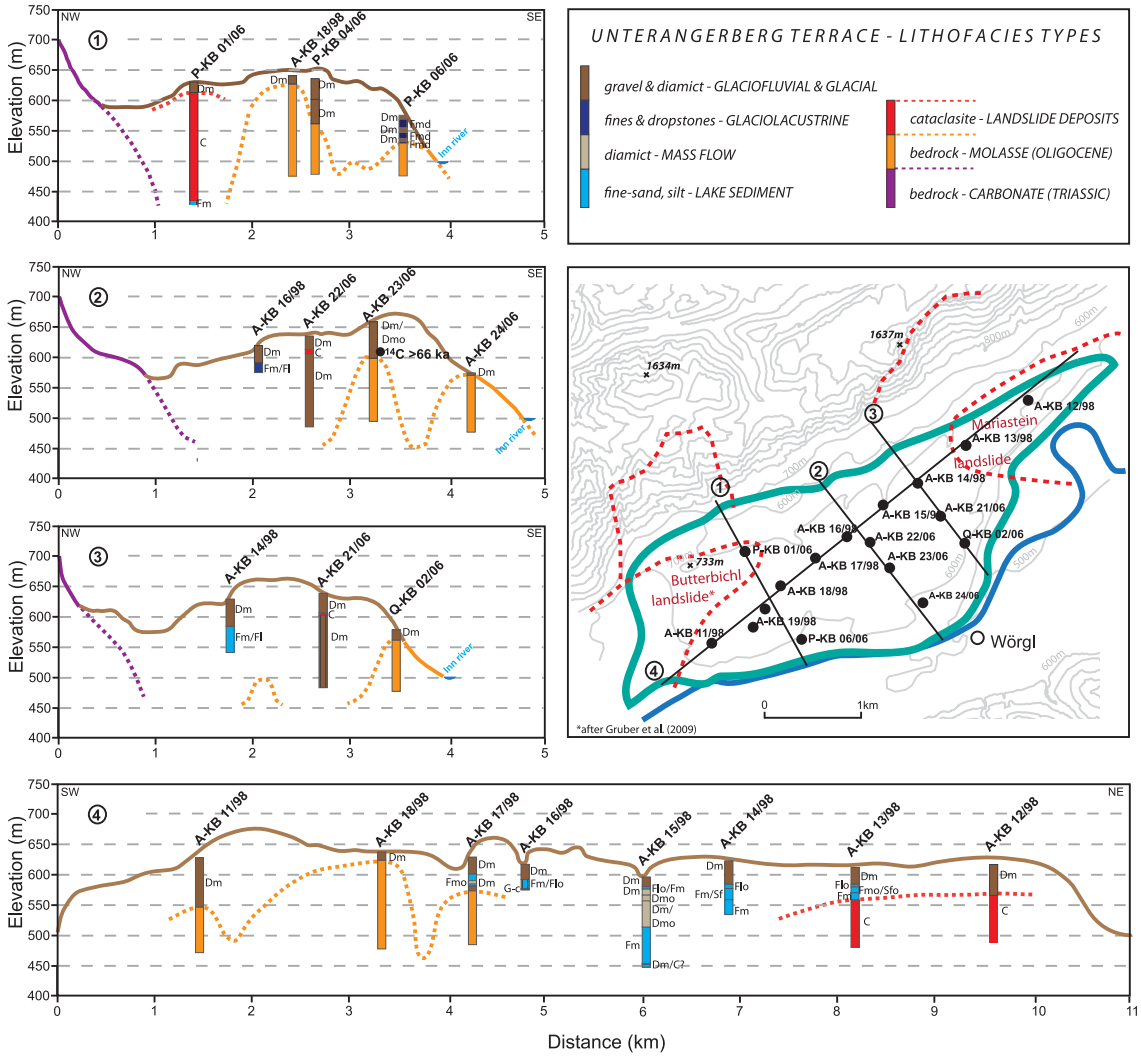

Fig. 3. Schematic cross-sections and simplified borehole lithologies across the Unterangerberg terrace including information from geophysical measurements (vertical exaggeration is 1:6.25). Dotted lines represent the paleo-surface topography (see Table 1 for lithofacies code descriptions).

according to Cushing (1964). Samples with a pollen sum <20 grains per slide were considered as pollen-free and are marked by a dotted line in the pollen diagram.

The organic sequences in core A-KB 17/98 (core depth 25.5–27.0 m; 41.5–41.9 m) are strongly compressed fine-detritus layers, mostly composed of Cyperaceae with scattered remains of mosses and wood particles. These peat layers were fairly resistant to chemical treatment, resulting in weak pollen enrichment and low pollen sums in the diagram. Thus the actual pollen content in the sediment is expected to be higher than counted.

3.3. Radiocarbon dating

A total of 34 wood and plant macro remain samples were collected from the cores and dated using ^{14}C (Table 3). Where possible, plant macro remains such as mosses and seeds were used, but most samples are wood fragments. Samples were prepared at the ^{14}CHRONO Centre, Queen's University Belfast, and analysed using acceleration mass spectrometry (AMS). MIS 7 kauri wood provided by A. Hogg, University of Waikato, was used for the background correction. Ages were calculated according to Stuiver and Polach (1977) using the AMS measured $^{13}C/^{12}C$ which accounts for both natural and machine isotope fractionation. Ages younger than 47 ka BP were calibrated using the IntCal09 (Reimer et al., 2009) calibration curve and the Calib 6.0 software (Stuiver et al., 2005). Calibrated ages are reported with a one standard deviation (1σ).

3.4. Luminescence dating

3.4.1. Sample preparation and analytical facilities

Because the drill cores (10.2–12.7 cm diameter) had been stored under normal daylight conditions for several years, only completely intact sections of the cores were sampled, i.e. mostly fine-grain sequences. All subsequent preparation and analysis steps were made under subdued red-light conditions in the laboratory. First, the outermost, light-exposed parts were gently removed by hand. Then, carbonate and organic contents were removed using hydrochloric acid (10%) and hydrogen peroxide (10%). In between and after these steps, samples were washed with distilled water. The polymineral fine-grain 4–11 μm fraction was extracted by repeated washing and centrifuging following Frechen et al. (1996). Luminescence measurements were made using an automated Risø TL/OSL DA-15 Reader equipped with a calibrated $^{90}Sr/^{90}Y$ beta source (~0.08 Gys^{-1}). For recording the feldspar signal from polymineral samples, aliquots were stimulated using infrared light (870 nm)

Table 1
Lithologies, lithofacies types and genetic interpretation of Pleistocene sediments from Unterangerberg terrace.

Lithology	Description	Lithofacies code	Genetic interpretation
Diamict	Matrix-supported, organic remains	Dmo	Mass flow deposit
	Matrix-supported, sterile	Dm	Glacial till
Gravel	Clast-supported, sub- to well rounded, striated clasts	Gc	Glaciofluvial sediment (topset)
	Clast-supported, monomictic, angular to sub-angular	Gc-c	Fluvial (re-deposited landslide cataclasite)
Sand	Massive/organic content	Sm/Smo	Fluvial deposition (topset)
	Laminated/organic content	Sl/Slo	Bottomset
	Monomictic, angular medium sand	Sc	Landslide deposit
Fines (fine-sand/silt/clay)	Massive	Fm	Distal delta foresets
	Laminated	Fl	Bottomset
	Organic remains (charcoal, plant detritus/mosses, pollen)	Fo	High aquatic and terrestrial productivity
	Dropstones	Fd	Glaciolacustrine deposition
Cataclasite	Angular limestone clasts, stones to boulders	C	Landslide deposit

diodes and the signal was recorded using a Schott BG39/Corning 7-59 filter combination.

3.4.2. Measurement protocol

The infrared stimulated luminescence (IRSL) signal obtained from polymineral fine-grain (4–11 μm) samples was measured using a single-aliquot regenerative-dose (SAR) protocol (Wallinga et al., 2000; Preusser, 2003) protocol. First, preheat plateau tests for temperatures between 160 and 310 °C were made, showing a plateau between 270 and 310 °C for all samples. Next, an additional measurement step at an elevated temperature of 225 °C as first introduced by Thomsen et al. (2008) was added in the SAR-protocol (so-called post-IR $IRSL_{225}$ or $pIRIR_{225}$) (Table 2) following the $IRSL_{50}$ measurement. This pIRIR signal is considered to have a high potential for minimising the degree of anomalous fading of the luminescence signal which is often reported from feldspar samples and, if not corrected for, leads to substantial age underestimation (cf. Aitken, 1998). For all samples, both the $IRSL_{50/225}$ and $pIRIR_{225}$ signal measurements yielded recycling ratios ranging between 0.9 and 1.1 and recuperation values <5%. To investigate the bleaching characteristics of the $IRSL_{50}$ and the $pIRIR_{225}$ signals, i.e. the time needed to reset the natural luminescence signal to zero under natural daylight conditions, a bleaching experiment was set up. Aliquots which received the same dose were exposed to direct sunlight for varying time periods (between 60 s and 120 min) and then measured using the protocol outlined above. The results showed that the $IRSL_{50/225}$ signal was bleached substantially faster (<5% after 20 min) than the $pIRIR_{225}$ signal (<5% after 120 min). Therefore, dose recovery tests were performed on all samples after sunlight exposure of minimum 2 h, with resulting values close to unity for both the $IRSL_{50/225}$ and the $pIRIR_{225}$ signals. Furthermore, in order to make clear whether the $IRSL_{50/225}$ and also the $pIRIR_{225}$ signals are affected by anomalous fading or not, fading tests were conducted on aliquots used for age calculations following Auclair et al. (2003), with storage times ranging between 30 min (prompt measurement) and ~7 days (delayed measurements). Anomalous fading is expressed as the *g*-value, representing the signal loss per decadce (Aitken, 1998) (for further details on the experimental setups see Starnberger et al., submitted for publication).

Table 2
IRSL-SAR protocol used for recording of the feldspar signal from fine-grain polymineral aliquots.

Step	Treatment	Observed
1	Give dose[a]	
2	Preheat (290 °C for 60 s)	
3	IR stimulation (50 °C for 300 s)	$L_n/L_x(IRSL_{50/225})$
4	IR stimulation (225 °C for 300 s)	L_n/L_x ($pIRIR_{225}$)
5	Give test dose	
6	Preheat (290 °C for 60 s)	
7	IR stimulation (50 °C for 300 s)	$T_n/T_x(IRSL_{50/225})$
8	IR stimulation (225 °C for 300 s)	$T_n/T_x(pIRIR_{225})$
9	Return to 1	

[a] For L_n this is 0.

For investigating the saturation behaviour of luminescence signals recorded, a single saturating exponential function was fitted for every aliquot in order to calculate $2D_0$ values. These are considered to represent the ~85% saturation threshold above which a dose is considered to be saturated and therefore should be excluded from any age calculations (Wintle and Murray, 2006). For calculating ages, equivalent dose (D_e) values from and $IRSL_{50/225}$ L_x/T_x values were used. The number of aliquots was between three and ten. Regeneration dose points were best fitted to a single exponential plus linear (SEPL) function.

3.4.3. Dosimetry

The concentration of dose rate relevant elements was determined using inductively coupled plasma mass spectrometry (ICP-MS; Preusser and Kasper, 2001). Alpha, beta, and gamma dose rate conversion factors were taken from Adamiec and Aitken (1998). A mean *a*-value of 0.07 ± 0.2 for the fine-grain polymineral samples was used (Rees-Jones, 1995; Lang et al., 2003; Preusser, 2003). Calculations of cosmic dose rate (DR) values were made after Prescott and Stephan (1982). Due to the fact that the sediment in the cores was completely desiccated, an estimated average water content value of 27% was calculated from sporadic measurements which were made during the drilling of the cores. To take past changes of moisture into account, an uncertainty of 10% was used for all samples.

4. Results and interpretation

4.1. Core description and lithofacies types

The analysis of the cores was hampered by the fact that some parts were disturbed during drilling: this was especially the case for gravel and sand units which – except for some fine sand units – were completely disturbed because drilling was performed without liners. Nevertheless, it was possible to define lithofacies types as a basis for genetic interpretations of the individual sediment types (see Table 1).

Each of the 17 cores studied in this work has an individual lithostratigrahpy, with great variation from core to core (Fig. 3), highlighting the complex stratigraphic pattern in the subsurface of

the Unterangerberg terrace. In the following, the most important lithofacies types as identified in the cores and illustrated in Fig. 3 are briefly described, starting with the pre-Quaternary base of the terrace.

The Tertiary bedrock was reached in several drillings (see Fig. 3). Among these, core A-KB 18/98 contains the longest Oligocene sequence, with 155.8 m of grey, middle- to fine-grained sandstone with intercalated greyish/brownish, silty to sandy marl as well as fine-grained mudstone. The same lithology is also present in other cores containing bedrock sequences (A-KB 11/98, A-KB 17/98; A-KB 23/06; A-KB 24/06; P-KB 04/06; P-KB 06/06; Q-KB 02/06).

On top of the bedrock, overconsolidated *diamict* was encountered in some of the drill holes (A-KB 11/98, A-KB 17/98, A-KB 18/98, A-KB 23/06, A-KB 24/06, P-KB 04/06, P-KB 06/06, Q-KB 02/06 – see Fig. 3). This sediment is massive, matrix-supported and unsorted or poorly sorted, with polymodal grain sizes ranging from fine silt to boulders. The roundness of the larger clasts ranges from angular to rounded; bullet-shaped and striated clasts are common. The clast spectrum comprises sedimentary (e.g. limestone, sandstone, marl) and metamorphic (e.g. quartzite, amphibolite, phyllite, gneiss) rock types. Some cores also retrieved diamict with sandstone, marl and mudstone clasts, probably derived from Tertiary rocks beneath.

In core A-KB 15/98, a complex series of different diamict layers at ~147–145.5 m and between ~64 and 22 m depth was encountered. At 147–145.5 m depth, the components are subrounded to rounded, with carbonate clasts embedded in a brownish matrix. This diamict is intercalated in between thick fine-grained silt layers. Between 78.0 and 74.0 m depth in the core, a similar diamict layer was found, with a strong organic smell reported during drilling. This layer is deposited on top of a long sequence of silt and topped by ~10 m of matrix-supported diamict with mixed limestone and crystalline clasts. Between ~64 and 22 m, there is a complex series of matrix-supported and clast-supported diamict layers with a matrix-supported layer of silty fine sand with subangular to subrounded clasts between 40 and ~35 m depth (565–560 m a.s.l.). Between ~35 and 22 m, there are subangular to rounded limestone and crystalline clasts. It is interesting to note in this core organic detritus was present at 147.5–147.0 m and 631.5–613.5 m. At 40.0 m and 38.1 m depths, pieces of wood were found.

Organic-bearing diamict is also present in core A-KB 17/98 between 40 and ~34 m depth: here, a matrix-supported diamict layer with subrounded to rounded and (partly) striated clasts contains pollen, wood and other plant macro-remains. In the same core, another such layer is present between 51.4 and ~44.0 m depth (i.e. 585.63–578.23 m a.s.l.): in the upper part, until ~46.3 m, it is matrix-supported with a brownish fine-grain sediment and some low pollen content; the subrounded to rounded, mostly crystalline clasts with diameters of up to ~20 cm show strong weathering features. Between ~ 51.4 and 46.3 m, the diamict is sterile and contains clasts derived from the Oligocene Angerberg Formation. A breccia composed of Angerberg Formation is present at the bottom of the core.

In core A-KB 23/06 (47–51 m depth/614.87–610.87 m a.s.l.) diamict with a brownish matrix was encountered which contained a wood fragment at 47.2 m.

Gravel is mostly clast-supported with a bimodal grain size distribution (sand and gravel). Clasts show different degrees of roundness ranging from subrounded to well-rounded. They are often striated (likely due to the drilling process) and poorly to well sorted, with diameters of up to ~30 cm. The lithological composition shows a mix of limestone and crystalline rocks. These gravels typically occur between ~580 and 630 m a.s.l., just below the final diamict layer that tops all sequences. In core A-KB 16/98, between 45.4 and 43.4 m (599.25–597.25 m a.s.l.), there is a monomictic layer of subrounded/rounded carbonate clasts. The sediment is clast-supported and contains fine-grain particles. Clast size is relatively homogenuous, with diameters ranging from ~2 to 5 cm.

Long *fine-grain sequences* were encountered in several drill holes. In cores A-KB 15/98 and P-KB 01/06 fine-grain sequences were penetrated at 450 and 428 m a.s.l., respectively. These are the lowest elevations reached by any of the cores, 150 (A-KB 15/98) and 202 m (P-KB 01/06) below the surface, or 50 and 72 m below the modern level of the Inn River, respectively. The lower sediments are greyish and dominated by fine sand to silt. The longest of these fine-grain sequences are found in the cores A-KB 14/98 and A-KB 15/98, where they are composed of massive, clayey to fine-sandy silt in the lower parts (A-KB 14/98: 85.0–62.5 m; A-KB 15/98: 145.5–78 m and 150.0–147.0 m depth) and of organic-rich, partly laminated silt in the upper parts (between ~583 and 577 m a.s.l.). The latter is further characterised by mollusc shell fragments, plant organic detritus and the presence of Characeae (stoneworts) remains (oospores and organic carbonate), with organic carbon content values between 1 and 10% (biogenic carbonate not included). Very similar organic-rich fine-sequences are also found in cores A-KB 13/98, A-KB 14/98, A-KB 16/98 and A-KB 17/98. In core A-KB 17/98, a sequence of a fine detritus gyttja (~44 and 43 m) and a calcareous gyttja (~43–42 m) topped by a lignite layer (~42.0–41.5 m) is present, overlying a diamict layer with some organic content (~46.5–44 m).

Organic-free, massive silt sequences with angular to subrounded dropstones are present in core P-KB 01/06 (198.8 and 194.8 m); subrounded to rounded dropstones were found in the massive fine-sandy silt section of core A-KB 15/98, between 74.0 and 64.10 m depth (535.48–525.58 m a.s.l.). Core P-KB 04/06 comprises several dropstone-rich units.

Long sequences of *cataclasite* dominate the lithology of the cores A-KB 12/98, A-KB 13/98 and P-KB 01/06. In core A-KB 13/98, the uppermost ~1.3 m of the cataclasite contains weathered clasts. Additionally, there is a ~2.5 m-thick layer of monomictic and cataclastic dolomite debris between 31.90 and 29.35 m depth (605.46–601.91 m a.s.l.) in core A-KB 21/06, with grain sizes ranging from coarse sand to boulders (the latter exceeding the drill core of the drill core). A mix of dolomitic cataclasite and diamict as described above is present in core A-KB 22/06, between ~616 and 608 m a.s.l.

4.1.1. Interpretation of lithofacies

Diamict covering most of the Angerberg terrace is interpreted as LGM lodgement till as it shares characteristics of other till occurrences in the Inn valley region (Penck and Brückner, 1909; von Klebelsberg, 1935). The gravels below are typical glaciofluvial sediments deposited in front of the advancing glacier during the LGM.

The diamict at the base of the fine-grain sequences in core A-KB 17/98 is also interpreted as till, but its stratigraphic position suggests a pre-LGM age.

Diamict containing plant macro remains or even larger amounts of pollen is a common lithofacies type which is interpreted as till redeposited as debris flows on the slopes containing a mixture of unweathered till (possibly of MIS 6 age), soil and vegetation. One large mass flow or a series of mass flows is probably reflected in the long diamict sequence of core A-KB 15/98. At this depth also the organic-free sections are interpreted as localized mud flow deposits since they cannot be traced across to the neighbouring core A-KB 14/98.

The different fine-grain sediments are interpreted as lacustrine deposits. The lower, massive deposits which locally contain small amounts of dropstones, probably formed during intervals of high sedimentation rates. In contrast to this, the laminated and

organic-rich sequences found in the upper parts of a number of cores point at rather slow sedimentation rates. The presence of Characeae macro remains (A-KB 1498, ~49.0–43.5 m; A-KB 15/98, ~22–18 m; A-KB 17/98, ~34–29 m, A-KB 16/98, ~40.8–33.7 m) indicates sedimentation in an oligo- to mesotrophic lake. The fine detritus gyttja – calcareous gyttja – lignite layer – sequence in core A-KB 17/98 (44–41.5 m depth) reflects the changing water level in the lake.

The long cataclastic sequences present in some cores are interpreted as deposits from two separate landslides as there is no sedimentary connection between the two depositional areas (Gruber, 2008). Both landslide deposits, however, are covered by till of the LGM (Penck and Brückner, 1909; Gruber, 2008; Gruber et al., 2009), thus providing a constraint on their minimum age. The western landslide deposit (referred to as Butterbichl landslide) is composed of cataclastically deformed dolomite (Upper Triassic Hauptdolomite Formation) from the mountain immediately north of the terrace (Gruber et al., 2009). It is dominated by a mixture of angular sand, stones and boulders, with sand dominating at the basis. While there is evidence from core P-KB 01/06 that this landslide entered a paleolake (Gruber et al., 2009), the base of the eastern landslide (Mariastein landslide) was not reached during coring. However, there is field evidence suggesting that also Mariastein went into a paleolake (Gruber, 2008). At Mariastein, the cataclastic facies is dominated by limestone and dolomite clasts from the Wetterstein Formation of the mountain to the north (Gruber et al., 2009). Short intervals of cataclastic dolomite are also present in cores A-KB 21/06 and A-KB 22/06 (see Fig. 3) and may be connected with the Butterbichl event. Further, the monomictic gravel layer in the lower part of core A-KB 16/98 is interpreted as a re-deposited landslide deposit because of its clast composition and deposition at ca 600 m a.s.l. This allows correlation with the Butterbichl cataclasite.

4.2. Radiocarbon dating

28 samples of plant macro remains from cores A-KB 14/98, A-KB 15/98, A-KB 16/98 and A-KB 17/98 were radiocarbon dated. Several samples from the older parts of the cores and from diamictic debris-flow deposits yielded infinite dates (Table 3). The data from the uppermost organic-rich lacustrine layer of core A-KB 17/98 (25.9–26.4 m) show age differences as large as ~15 ka within 50 cm. Different ages are also present deeper down in the same core, between 31.9 and 31.4 m.

4.2.1. Interpretation of radiocarbon data

Sampling explicitly concentrated on fossil wood and moss fragments as well as on seeds. Therefore, the effect of "dead carbon" incorporated in water plants during growth which may lead to erroneously old ages, is excluded. As a consequence, we regard the younger ages within a section as more reliable, as well as radiocarbon ages produced on mosses and seeds which are (i) undoubtedly of terrestrial (rather than aquatic) origin, and (ii) rule out possible re-deposition of older material as they are highly fragile.

Taken together, the radiocarbon data indicate deposition of the youngest lacustrine sediments between ~55 and 45 cal ka BP. The youngest radiocarbon ages in core A-KB 16/98 are from a fine-sand layer that may have been deposited outside the lacustrine

Table 3
Radiocarbon ages obtained from plant macro remains found in cores from the Unterangerberg terrace, w = wood, pd = plant detritus (indet.), m = mosses, s = seeds. Calibrated ages are given with one sigma uncertainty range.

Drill core	Depth (m)	UBA no.	Material	$\delta^{13}C$ (‰)$_{VPDB}$	^{14}C age yrs BP	Error	cal ka BP (1σ)
A-KB 14/98	45.7	UBA-18228	pd	−15.3	41,098	1107	45.6–44.0
A-KB 15/98	38.1	UBA-10869	w	−21.8	>52,148		
		UBA-10870	w	−22.6	>53,634		
	40	UBA-18232	w	−20.8	>52,165		
A-KB 16/98	29.8	UBA-11690	w	−25.4	35,319	374	41.1–40.1
	29.9	UBA-10872	w	−27.8	35,466	486	41–40.1
	32.2	UBA-15795	w	−28.3	42,301	1013	46.3–44.8
	37	UBA-14420	w	−30.7	>49,579		
	40.8	UBA-17190	m	−24.7	>47,636		
	41.5	UBA-14421	w	−29.8	>51,778		
	45.0	UBA-14422	w	−28.0	>55,414		
	45.2	UBA-14423	w	−29.4	>51,778		
	45.5	UBA-14424	w	−30.0	>51,778		
	46	UBA-14425	w	−32.5	>51,778		
A-KB 17/98	25.9	UBA-10874	w	−29.4	40,193	824	44.7–43.4
	26	UBA-11845	w	−26.7	40,512	698	44.9–43.8
	26.4	UBA-11846	w	−27.5	49,153	2232	–
		UBA-10873	w	−29.4	50,598	1716	–
	31.4	UBA-15796	pd	−29.8	>50,028		–
	31.6	UBA-11684	pd	−28.8	43,679	1169	48.1–45.7
	31.9	UBA-15797	w	−28.3	51,386	3233	–
	37.9	UBA-14426	w	−28.6	>53,800		
	38.1	UBA-18230	w	−27.6	>52,165		
		UBA-11685	w	−27.1	>54,229		
	38.7	UBA-17608	s	−32.5	47,459	3794	–
	39.9	UBA-18231	m	−19.4	32,518	409	37.6–36.6
		UBA-20031	m	−25.7	44,031	1840	46.9–43.8
		UBA-20032	m	−25.9	44,518	1943	47.4–44.2
	41.8	UBA-11686	w	−25.0	>54,394		
	42.5	UBA-11687	w	−26.4	>58,136		
	43.65	UBA-11688	w	−23.7	>58,136		
	46.1	UBA-11689	w	−25.8	>54,322		
A-KB 23/06	47.2	UBA-10875	w	23.8	>53,634		
		UBA-10876	w	28.9	>53,634		

environment. The anomalously young age at A-KB 17/98 at 39.9 m is considered the result of contamination.

4.3. Luminescence dating

While environmental dose rates are relatively low for samples from the upper lacustrine sequences deposited between ~600 and 580 m a.s.l. (~2–3 Gy/ka), higher values are obtained from the fine-grain sections deposited at depths of ~565 m a.s.l. and below (~4-5 Gy/ka). While other studies on alpine and pre-alpine deposits report dose rates range between ~2 and 4 Gy/ka for fine-grain loess (e.g. Preusser and Fiebig, 2009; Thiel et al., 2011) and lake sediment samples (e.g. Dehnert et al., 2012), values of up to ~7 Gy/ka were determined for some inner-alpine sites (e.g. Klasen et al., 2007; Lukas et al., 2012). This general observation of relatively high dose rate values in the alpine realm can be explained by the strong influence of the (mostly crystalline) rocks from the Central Alps. A representative regeneration dose growth curve for one of the oldest samples (core A-KB 15/98, 152.0 m) from Unterangerberg is shown in Fig. 4, along with a decay curve (inlet) of the natural signal.

Anomalous fading tests conducted on both the $IRSL_{50/225}$ and the $pIRIR_{225}$ signals resulted in minor (i.e. average g-values of ~1.5% or below) or no fading for the $pIRIR_{225}$, but also for the $IRSL_{50/225}$ signal (Fig. 5). The $pIRIR_{225}$ equivalent doses and calculated ages, however, are distinctively larger than those from the $IRSL_{50/225}$ signal. Considering the low fading rates which make anomalous fading of the $IRSL_{50/225}$ unlikely to explain this observation, the $pIRIR_{225}$ seems to be affected by residual doses. Considering the results of the bleaching experiment as outlined in Section 3.4.2, this is not surprising as the experiment shows that the $pIRIR_{225}$ signal is distinctively harder to bleach than the $IRSL_{50/225}$ signal. Therefore, the $IRSL_{50/225}$ signal was used for age calculations.

The luminescence ages from all samples range between ~115 and ~45 ka and are generally stratigraphically consistent within their uncertainties, i.e. there are no age inversions in any of the cores. Generally, $2D_0$ values vary between 500 and 600 Gy, and D_e values used for dating range from ~125 to slightly below 500 Gy. Equivalent dose values of all samples and calculated ages are listed together with dosimetry data in Table 4 and are illustrated in Fig. 6.

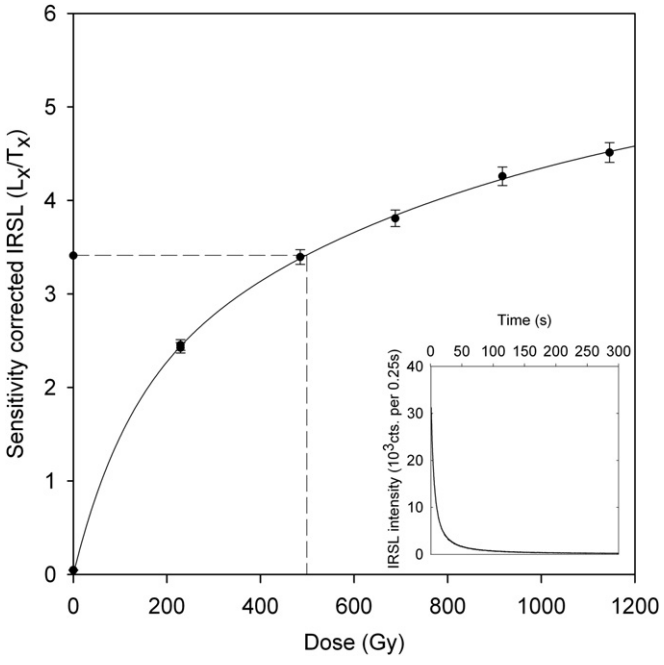

Fig. 4. Dose response curve generated from regeneration doses of up to 1150 Gy for core sample P-KB 01/06 (198.65 m).

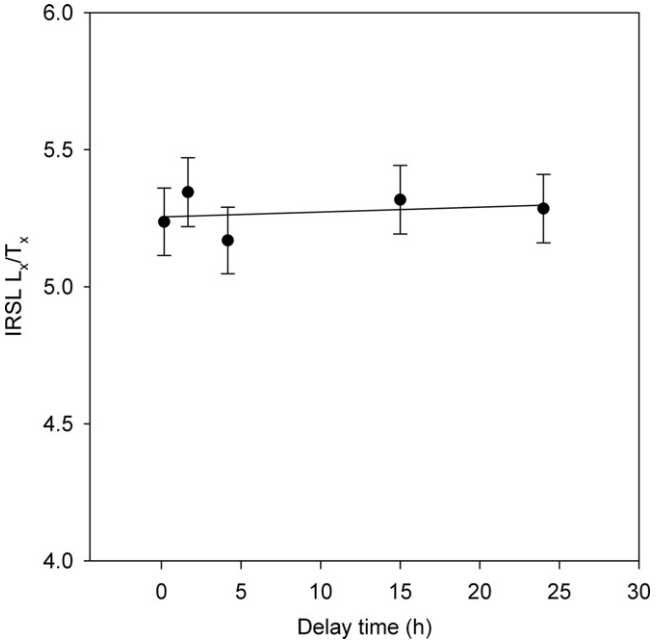

Fig. 5. Plot of storage time versus sensitivity-corrected IRLS L_x/T_x values obtained from an aliquot from core sample A-KB 15/98 (152.0 m) illustrating the absence of anomalous fading.

4.3.1. Interpretation of luminescence data

The IRSL ages from the Unterangerberg cores form three clusters which help to define three different lake phases (Fig. 6). Considering the uncertainty rages of the data, the first lake phase was deposited between ~125 and 90 ka. These oldest sediments are present in the lowest parts of cores A-KB 14/98, A-KB 15/98 and P-KB 01/06 which are all located at elevations of ~540–430 m a.s.l. in the central and deepest part of the paleobasin (see Fig. 3). The sediment consists of massive, organic-free silt with relatively high deposition rates indicated by the luminescence ages. At drill site A-KB 15/98, ~70 m of sediment were deposited between ~150 and 80 m depth, with luminescence data showing no clear trend of increasing age from top to bottom, which leads to the assumption of high depositional rates.

Evidence of a second lacustrine phase is present in cores A-KB 13/98 and A-KB 14/98, dated at ~70–60 ka, and possibly in core A-KB 12/98 at the same elevation, but no IRSL dates could be obtained from the sand layer in this core. The gap between ~100 ka at 62.5 m and 65 ka at ca 55 m depth in core A-KB 14/98 coincides with a rather sharp lithological transition from clayey to fine-sandy silt at ~60 m depth. In core A-KB 13/98, silt dated to ~70–60 ka was deposited on top of cataclasite from the Mariastein landslide event, with a potential paleosol suggested by weathering of the clasts in the top ~4 m. The sediment of this second lake phase, which coincides with the MIS 4, again suggests cold climatic conditions due to high deposition rates and the absence of organic material. No evidence of the presence of direct glacial influence during this time period was found in the sediments. This is in agreement with information from Samerberg (Grüger, 1979) and Mondsee (Drescher-Schneider, 2000; Krenmayr, 2000), two key sites at the northern margin of the Eastern Alps, which also lack evidence for a MIS 4 lowland glaciation. Such a glaciation, however, has been reported for the Western Alps (e.g. Welten, 1982;

Table 4
Summary of luminescence and dosimetry data used for OSL-dating of fine-grain sediments from cores at the Unterangerberg terrace, with core names, sample depths, concentrations of dose rate relevant elements (U, Th, K), dose rate (DR), equivalent dose (D_e) and resulting ages.

Sample	Depth (m)	U [ppm]	Th [ppm]	K [%]	DR	D_e	Age (ka)
A-KB13/98	38.7	3.00 ± 0.30	9.90 ± 0.99	1.83 ± 0.18	3.21 ± 0.22	199.4 ± 14.6	62 ± 7
	43.1	4.00 ± 0.40	9.40 ± 0.94	1.66 ± 0.17	3.36 ± 0.24	217.5 ± 6.1	65 ± 5
	50.2	3.50 ± 0.40	10.60 ± 1.10	2.4 ± 3.84	3.84 ± 0.25	260.0 ± 23.1	68 ± 8
A-KB 14/98	54.85	4.10 ± 0.41	15.00 ± 1.50	2.51 ± 0.25	4.51 ± 0.29	293.3 ± 7.9	65 ± 5
	62	4.10 ± 0.41	12.70 ± 1.27	3.10 ± 0.31	4.77 ± 0.32	504.1 ± 49.9	106 ± 13
	70	4.00 ± 0.40	12.50 ± 1.25	2.62 ± 0.26	4.35 ± 0.28	429.6 ± 31.2	99 ± 10
	74	4 ± 0.40	12.50 ± 1.30	2.9 ± 0.30	4.63 ± 0.29	482.2 ± 44.5	104 ± 12
	78	3.6 ± 0.36	13.60 ± 1.36	3.20 ± 0.32	4.77 ± 0.30	527.3 ± 56.1	111 ± 14
	82	3.6 ± 0.36	13.60 ± 1.36	2.62 ± 0.26	4.84 ± 0.30	507.7 ± 34.4	106 ± 8
A-KB 15/98	17.4	2.60 ± 0.23	11.00 ± 1.10	2.65 ± 0.26	3.82 ± 0.25	167.5 ± 12.8	44 ± 4
	21.7	3.70 ± 0.37	11.20 ± 1.12	2.84 ± 0.28	4.28 ± 0.28	234.3 ± 11.7	55 ± 5
	66.7	4 ± 0.40	12.60 ± 1.26	2.48 ± 0.25	4.25 ± 0.28	390.5 ± 23.4	92 ± 8
	69.85	3.5 ± 0.35	11.60 ± 1.16	2.67 ± 0.27	4.16 ± 0.27	492.0 ± 35.5	118 ± 12
	79.15	3.7 ± 0.37	12.90 ± 1.29	2.6 ± 0.26	4.28 ± 0.28	486.4 ± 31.4	114 ± 10
	117	3.8 ± 0.38	11.50 ± 1.15	2.72 ± 0.27	4.29 ± 0.28	461.4 ± 34.1	108 ± 11
	143	3.5 ± 0.35	11.30 ± 1.13	2.81 ± 0.28	4.24 ± 0.27	476.4 ± 35.2	112 ± 11
	152	4.2 ± 0.42	13.30 ± 1.33	2.73 ± 0.27	4.57 ± 0.18	499.8 ± 54.8	110 ± 13
A-KB16/98	32.2	3.00 ± 0.30	7.90 ± 0.79	2.70 ± 0.27	3.70 ± 0.25	172.3 ± 9.3	48 ± 4
	37	3.70 ± 0.37	9.10 ± 0.91	2.64 ± 0.26	3.98 ± 0.26	172.0 ± 5.2	41 ± 3
	38.3	4.60 ± 0.46	12.00 ± 1.20	2.85 ± 0.29	4.67 ± 0.29	223.1 ± 0.5	45 ± 4
	40.8	3.8 ± 0.38	8.60 ± 0.86	2.26 ± 0.23	3.68 ± 0.25	162.8 ± 7.1	42 ± 3
	45.6	3.70 ± 0.37	7.40 ± 0.74	2.32 ± 0.23	3.61 ± 0.24	194.3 ± 8.4	54 ± 4
A-KB17/98	30.2	3.00 ± 0.30	8.50 ± 0.85	1.64 ± 0.16	2.59 ± 0.21	139.1 ± 6.3	54 ± 5
	31.6	3.80 ± 0.38	6.00 ± 0.60	1.66 ± 0.17	2.98 ± 0.22	138.6 ± 6.9	47 ± 4
	34.2	2.60 ± 0.26	10.70 ± 1.07	2.03 ± 0.20	3.31 ± 0.23	171.7 ± 13.4	52 ± 5
	42.5	2.92 ± 0.29	7.58 ± 0.76	1.37 ± 0.14	2.65 ± 0.17	131.3 ± 5.1	50 ± 4
	42.8	2.67 ± 027	8.12 ± 0.81	1.42 ± 0.14	2.66 ± 0.22	141.4 ± 2.6	53 ± 4
P-KB 01/06	198.65	3.6 ± 0.36	11.3 ± 1.13	2.58 ± 0.26	4.07 ± 0.27	462.1 ± 16.2	114 ± 8
	201.9	3.5 ± 0.35	11.1 ± 1.11	2.42 ± 0.24	4.02 ± 0.26	460.2 ± 17.4	115 ± 9

Schlüchter, 1991; Keller and Krayss, 1998; Link and Preusser, 2005; Preusser et al., 2007).

The youngest, IRSL-dated lake phase at Unterangerberg occurred during MIS 3, as indicated by luminescence and calibrated radiocarbon data which are in stratigraphic agreement with each other. At this time the basin was already filled with Pleistocene deposits up to ~575 m a.s.l. IRSL dates range between ~52 and 43 ka and are in general agreement with early MIS 3 IRSL ages from other lacustrine (e.g. Link and Preusser, 2005; Klasen et al., 2007; Preusser and Degering, 2007; Anselmetti et al., 2010; Dehnert et al., 2012; Lowick et al., 2012) and loess (e.g. Preusser and Fiebig, 2009; Thiel et al., 2010, 2011) deposits in and north of the Alps. Sediments of this third paleolake are preserved in cores A-KB 13/98, A-KB 14-98, A-KB 15/98, A-KB 16/98 and A-KB 17/98, indicating that this lake had probably a larger extent than the two previous ones. Abundant zoological and botanical remains found in the mostly laminated silt indicate a rich aquatic ecosystem under interstadial conditions.

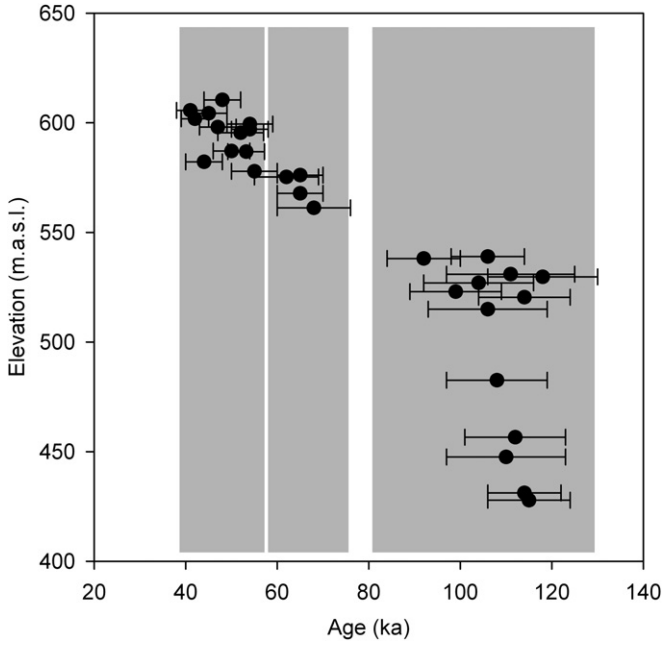

Fig. 6. Time vs. elevation plot of the IRSL results obtained from fine-grain lacustrine sequences at Unterangerberg, illustrating three lake phases and elevation levels.

4.4. Pollen record

The palynological investigations yielded a detailed picture of changing environmental conditions as reflected in the vegetation composition, ranging from dense coniferous forests to open grass tundra. In the following, local pollen zones (LPZ) are described for each core along an E–W-transect.

4.4.1. A-KB 13/98

Three of five samples from this core were pollen free. The remaining samples rendered analysis difficult due to the presence of HF-resistant minerals such as zircon. The lowermost samples at 51.51 and 46.05 m have low pollen sums and concentration values, with arboreal percentages of 17 and 26%, respectively. *Pinus* is the dominant species of 8.3 and 10.0%, respectively. The non-arboreal pollen spectrum is dominated by grasses (Poaceae) and sedges (Cyperaceae). Due to these results and the rather homogenous lithology of the fine-grain sections of this core, no further samples were analysed.

4.4.2. A-KB 14/98

Four samples were investigated, with the uppermost sample (43.5 m core depth) being pollen-free. The two lowermost samples at 50.20 and 48.35 m show a dominance of *Pinus* (28 and 41%, respectively), with the arboreal pollen percentage of 58% in sample 48.35 m being only slightly below the threshold of 60% for forest vegetation. The sample from 46.30 m has arboreal values of 31%, dominated by *Betula* with 22% followed by *Pinus* with 6%.

4.4.3. A-KB 15/98 (Fig. 7a and b)

The sandy/silty lacustrine sequence between 15.5 m and 22.0 m as well as the organic-free, massive silt between ~79 and 152 m depth were analysed. The samples of the upper part of this core (19.4–16.0 m) yielded generally low pollen concentration values ranging between ~1000 grains/ml (17.2 m) to ~40,000 grains/ml (19.0 m), whereas the pollen concentration reached values between 15,000 (20.3 m) and 280,000 grains/ml (20.0 m) in the middle part. Some sections, however, are pollen-free (at 21.2, 21.6, 38.5, 52.7, 66.7, 79.1, 117.0, 143.0 and 152.0 m).

4.4.3.1. LPZ KB 15-1 (52.7 m): Picea- zone with Osmunda. This pollen zone consists of one sample collected in an organic-rich section of a thick diamictic layer. The total arboreal pollen content of >90% indicates a dense forest vegetation with 60% of *Picea* pollen. This dominance of spruce, along with low percentages of thermophilous tree species as well as spores of *Osmunda*, allows to correlation of this sample with pollen zone PZ KB 17-2 (see below). The diamictic material above and below this sample contains no organic material.

4.4.3.2. LPZ KB 15-2 (20.4–19.55 m, 9 samples): Betula–Pinus cembra–Juniperus zone. This zone is characterised by high pollen concentration values. The arboreal pollen contribution is as high as ~80%, with a dominance of *Betula* (up to 60%) and an almost continuous presence of low *Pinus cembra* (Swiss Pine) values. Further arboreal species are *Pinus*, *Picea*, *Alnus*, *Larix*, *Hippophaë*, *Juniperus* and *Ephedra*. Small amounts of *Quercus* and *Tilia* are considered to represent long-term transport or reworking of older sediment. The herb spectrum is diverse, with Apiaceae, Cichorioideae, *Helianthemum,* Ranunculaceae, Caryophyllaceae and others. Among the zoological micro-remains, oocysts of Neorhabdocoela (flatworm order) such as *Microdalyellia armigera* and the rare findings of *Gyratrix hermaphroditus* and *Strongylostama radiatum* are noteworthy.

4.4.3.3. LPZ KB 15-3 (19.55–16.60 m, 8 samples): herb zone. At ~19.5 m there is a drop in the arboreal pollen percentages to values <40% and in the overlying 20 cm to <20%. The remaining parts of this pollen zone show high non-arboreal pollen percentages dominated by grasses (Poaceae) and sedges (Cyperaceae) and *Artemisia*. Other herbs including Chenopodiaceae, *Thalictrum*, *Helianthemum*, and Cichorioideae contribute to this moderately diverse vegetation spectrum. The rare presence of *Glomus*, a fungus growing on bare soil, and pre-Quaternary sporomorphs like Pinaceae, trilet spores, and Hystrichospaeridae indicate high input of allochthonous material due to sparse vegetation cover.

4.4.4. A-KB 16/98 (Fig. 8a and b)

In this core, the sequence between 41.5 and 30 m was continuously sampled at 0.1–0.4 m intervals. Further samples were collected at 45.6, 43.2, 42.8, 42.5 and 42.2 m. The pollen concentration in this sediment is distinctively lower than for instance, in A-KB 15/98, ranging between ~400 and 9000 grains/ml. However, these values vary widely throughout cored section, from zero to >90,000 pollen grains/ml.

4.4.4.1. LPZ KB 16-1 (41.5–40.9 m): Pinus–Picea zone with Betula, Salix and Cyperaceae. Arboreal pollen percentages in this zone range between 30 and 60%, with *Pinus*, *Picea*, *Betula* and *Salix*. High proportions of grasses (Poaceae) and sedges (Cyperaceae) were observed, next to a relatively diverse herbal flora. Moss fragments and *Gaeumannomyces*, a fungal parasite living on *Carex*, indicate a lakeshore habitat.

4.4.4.2. LPZ KB 16-2 (40.9–38.0 m): treeless zone with partly very low pollen concentrations. Arboreal pollen percentages are low and the herbal pollen spectrum is dominated by Poaceae and *Artemisia*. In the upper part of the zone, at ~39–38 m depth, the pollen concentration increases slightly and a rich aquatic fauna and flora appears, indicating improving ecological conditions. A high amount of butterfly wing scales in the sample at 39.5 m depth, which is pollen-free, is noteworthy.

4.4.4.3. LPZ KB 16-3 (38.0–36.5 m): Betula–Juniperus–Pinus cembra zone. In this zone high pollen concentration values of up to 80,000 grains/ml were observed. Low birch values are accompanied by *Pinus*, *Juniperus* and *Pinus cembra*. *Picea* is almost entirely absent. Herbal and aquatic species are abundant. However, compared to the previous pollen zone, *Artemisia* values are low.

4.4.4.4. LPZ KB 16-4 (36.5–33.0 m): Pinus–Betula zone with Cichorioideae. In this zone arboreal pollen values remain low, ranging at values between ~15 and 30%, thus indicating an open landscape with little presence of trees and conditions remaining in favour of a relative diverse herbal flora and aquatic organisms. However, pre-Quaternary sporomorphs increased indicating a slowly shrinking vegetation cover.

4.4.4.5. LPZ KB 16-5 (33.0–31.4 m): Pinus–Betula zone with Cichorioideae. Compared to the previous zone, arboreal values slightly increase in this zone, with ~40% at 32.5 m. The tree species spectrum is reduced to *Pinus* and *Betula*. *Picea*, *Pinus cembra* and *Salix* disappeared. The herbal diversity is very poor, and so is the diversity of aquatic organisms. Remarkably, high amounts of pre-Quaternary sporomorphs which clearly outnumber the concentration of the pollen grains indicate increasing sedimentation of allochtonous material as a consequence of a decreasing vegetation cover due to less favourable environmental conditions.

4.4.4.6. LPZ KB 16-6 (31.4–30.2 m): zone with herbs and moss remains. Arboreal pollen values decrease again to ~30% and *Pinus* and *Betula* are accompanied by very small percentages of *Picea*. The herbal flora, however, recovered its diversity slightly, as well as the aquatic taxa. The number of pre-Quaternary sporomorphs remains high. In this zone, relatively high amounts of moss leaves were found. Pollen concentration values reach a minimum in this zone but show large changes: the samples between 28.3 and 29.5 m contain no pollen, while the sample from directly below, at 29.7 m, contains ~22,000 grains/ml. At 29.9 m, the concentration drops again to 383 grains/ml.

4.4.5. A-KB 17/98 (Fig. 9a and b)

This core offers probably the most complete pollen sequence. 63 samples were analysed between 25.95 and 46.2 m depth, with a gap from 26.42 to 30.10 m due to core loss during drilling.

4.4.5.1. LPZ KB 17-1 (46.2–44.65 m): forest with Pinus cembra, Pinus and Betula. This zone shows arboreal pollen percentages of almost 90%, with forest vegetation mostly composed of *Pinus* (generally >60%) and *Pinus cembra* (up to 35%). *Pinus* stomata are abundant, as well as pits of Pincaceae and charcoal. *Picea* is present with values

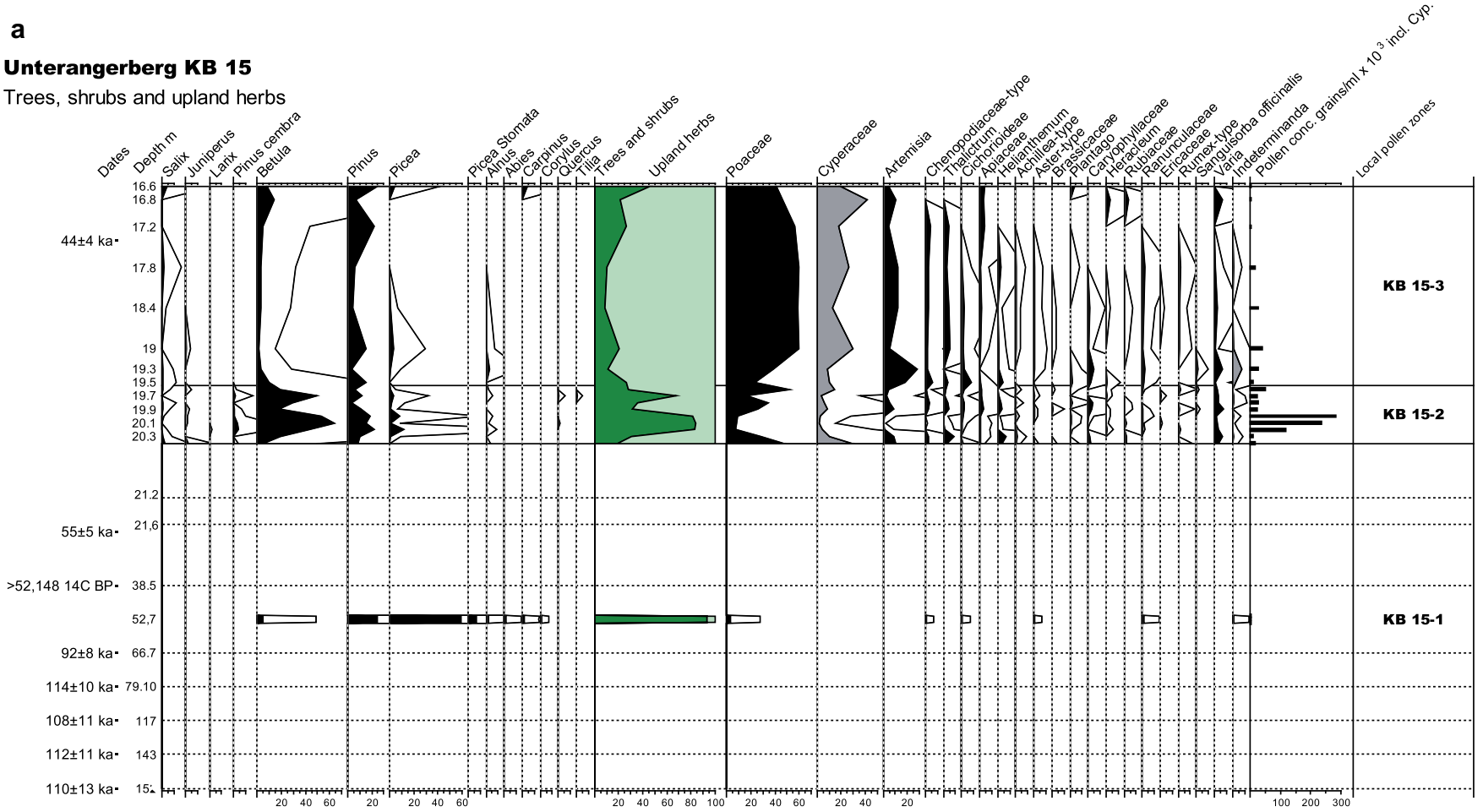

Fig. 7. a: Reduced pollen diagram of core A-KB 15/98 with the most important trees, shrubs, and upland herbs and selected dates. The thin black lines represent the pollen percentages (10× exaggerated). Taxa shown as gray curves are excluded from the pollen sum. Dates indicated as ka are OSL-dates, those indicated as BP are radiocarbon ages. b: Reduced pollen diagram of core A-KB 15/98 with the most important Pteridophyta and NPP and selected dates. The thin black lines represent the pollen percentages (10× exaggerated). Taxa shown as gray curves are excluded from the pollen sum. Dates indicated as ka are OSL-dates, those indicated as BP are radiocarbon ages.

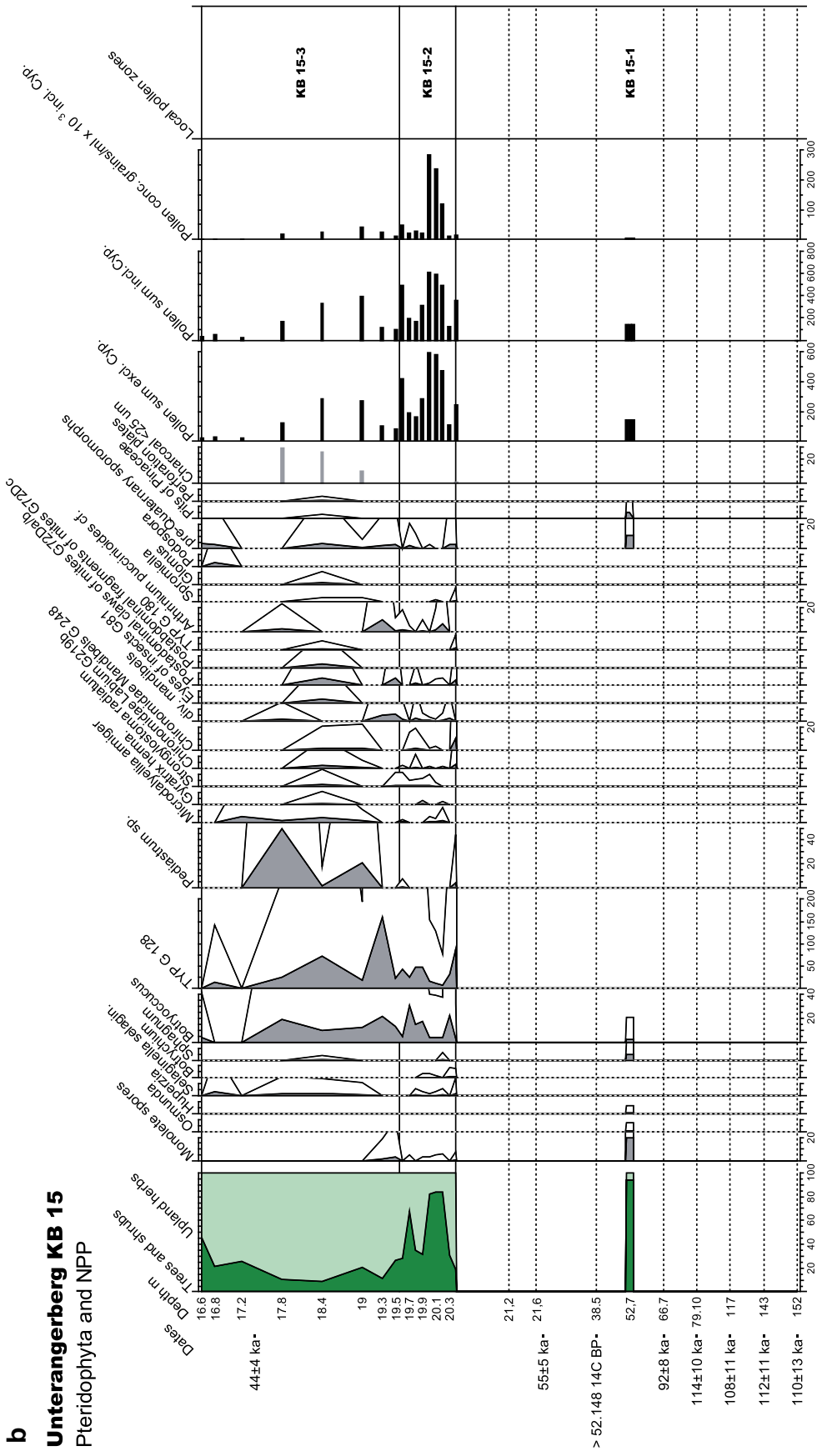

Fig. 7. (*continued*).

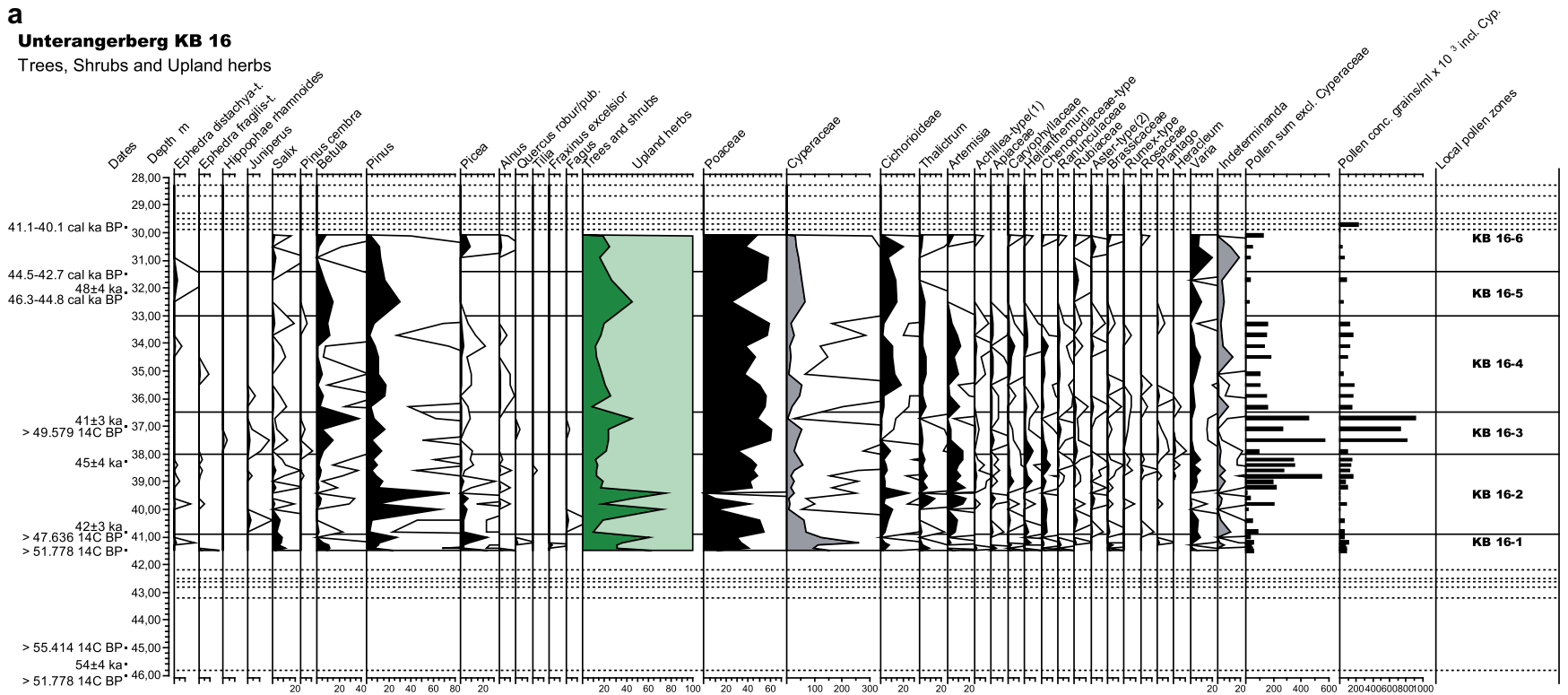

Fig. 8. a: Reduced pollen diagram of core A-KB 16/98 with the most important trees, shrubs and upland herbs and selected dates. The thin black lines represent the pollen percentages (10× exaggerated). Taxa shown as gray curves are excluded from the pollen sum. Dates indicated as ka are OSL-dates, those indicated as BP are radiocarbon ages. b: Reduced pollen diagram of core A-KB 16/98 with the most important Pteridophyta and NPP and selected dates. The thin black lines represent the pollen percentages (10× exaggerated). Taxa shown as gray curves are excluded from the pollen sum. Dates indicated as ka are OSL-dates, those indicated as BP are radiocarbon ages.

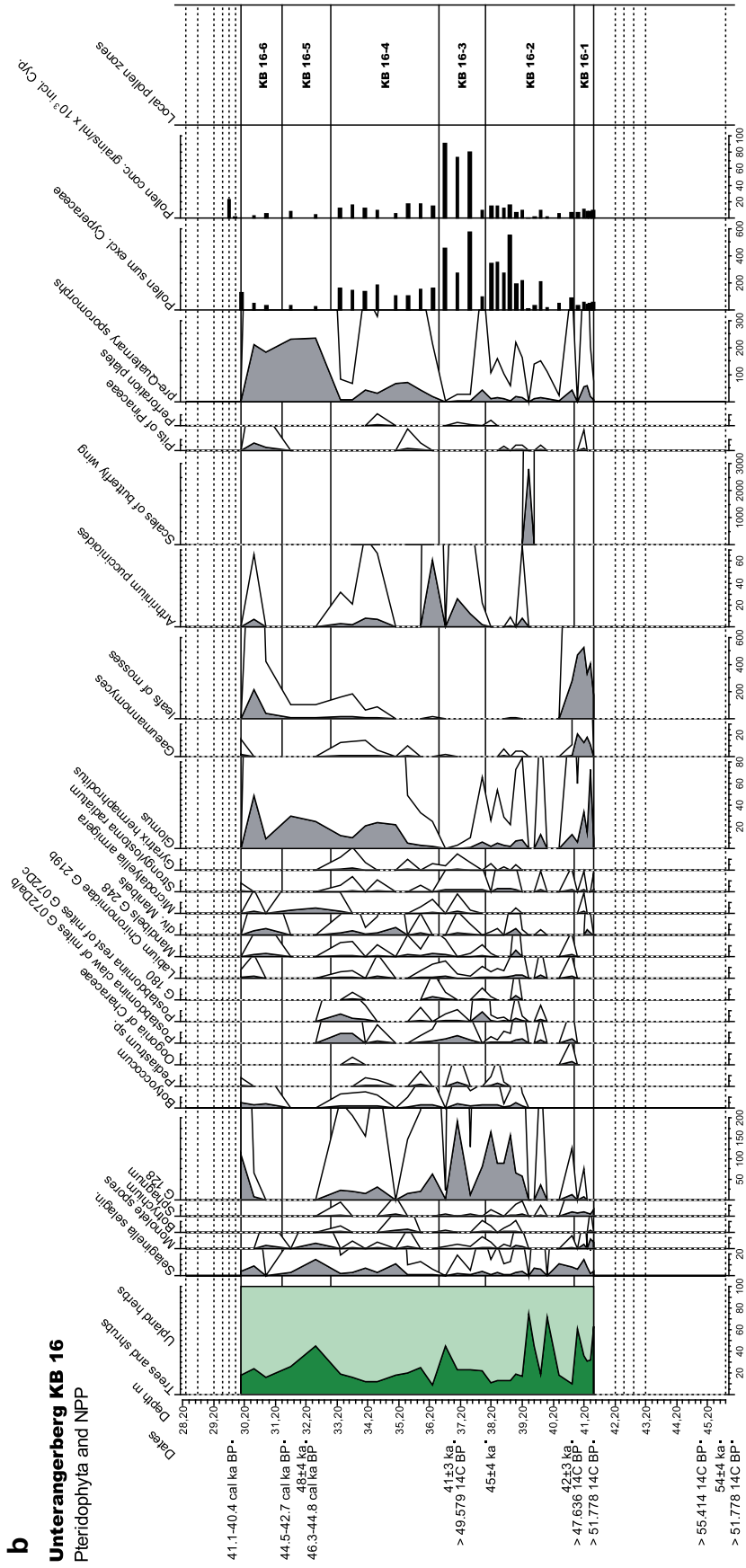

Fig. 8. (*continued*).

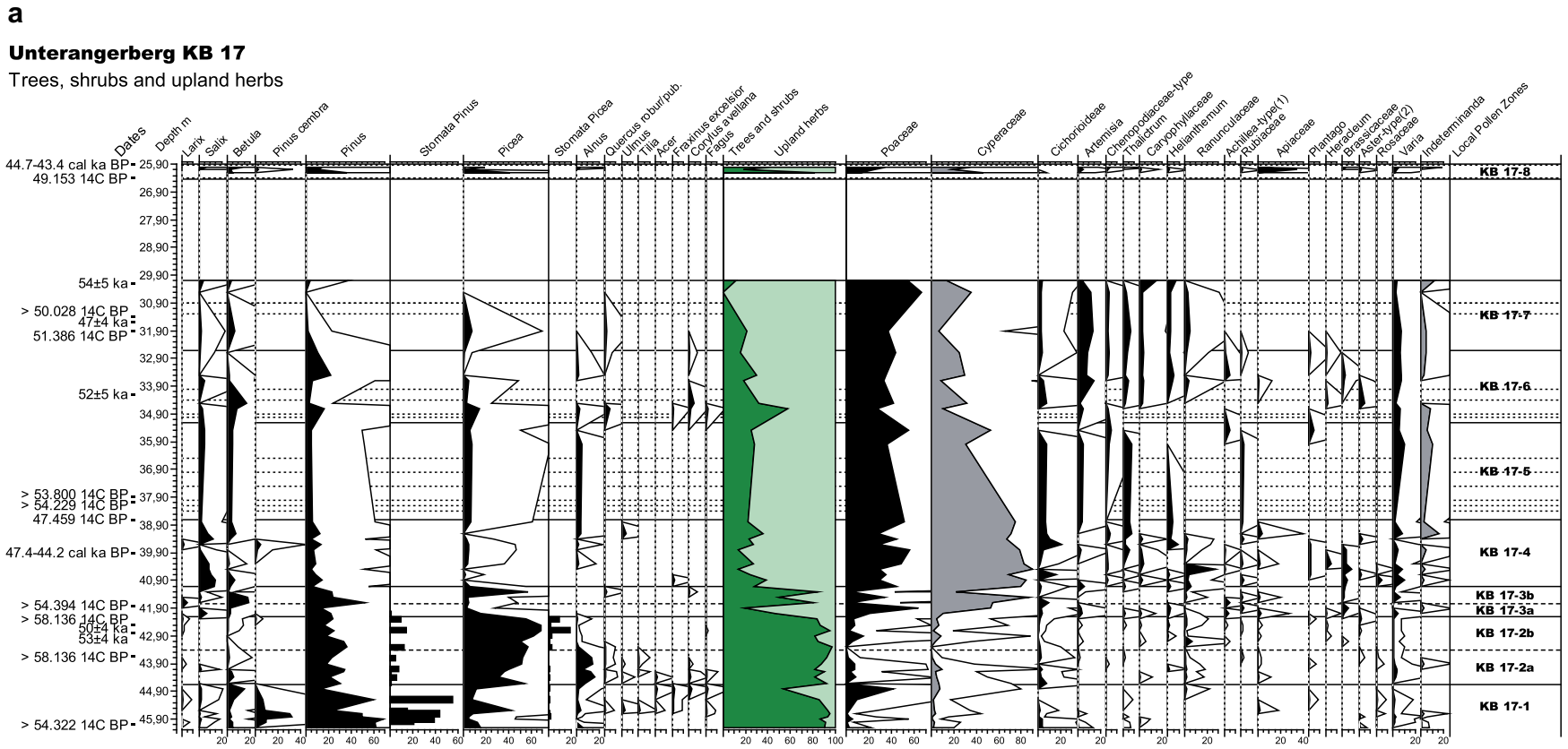

Fig. 9. a: Reduced pollen diagram of core A-KB 17/98 with the most important trees, shrubs and upland herbs and selected dates. The thin black lines represent the pollen percentages (10× exaggerated). Taxa shown as gray curves are excluded from the pollen sum. Dates indicated as ka are OSL-dates, those indicated as BP are radiocarbon ages. b: Reduced pollen diagram of core A-KB 17/98 with the most important Pteridophyta and NPP and selected dates. The thin black lines represent the pollen percentages (10× exaggerated). Taxa shown as gray curves are excluded from the pollen sum. Dates indicated as ka are OSL-dates, those indicated as BP are radiocarbon ages.

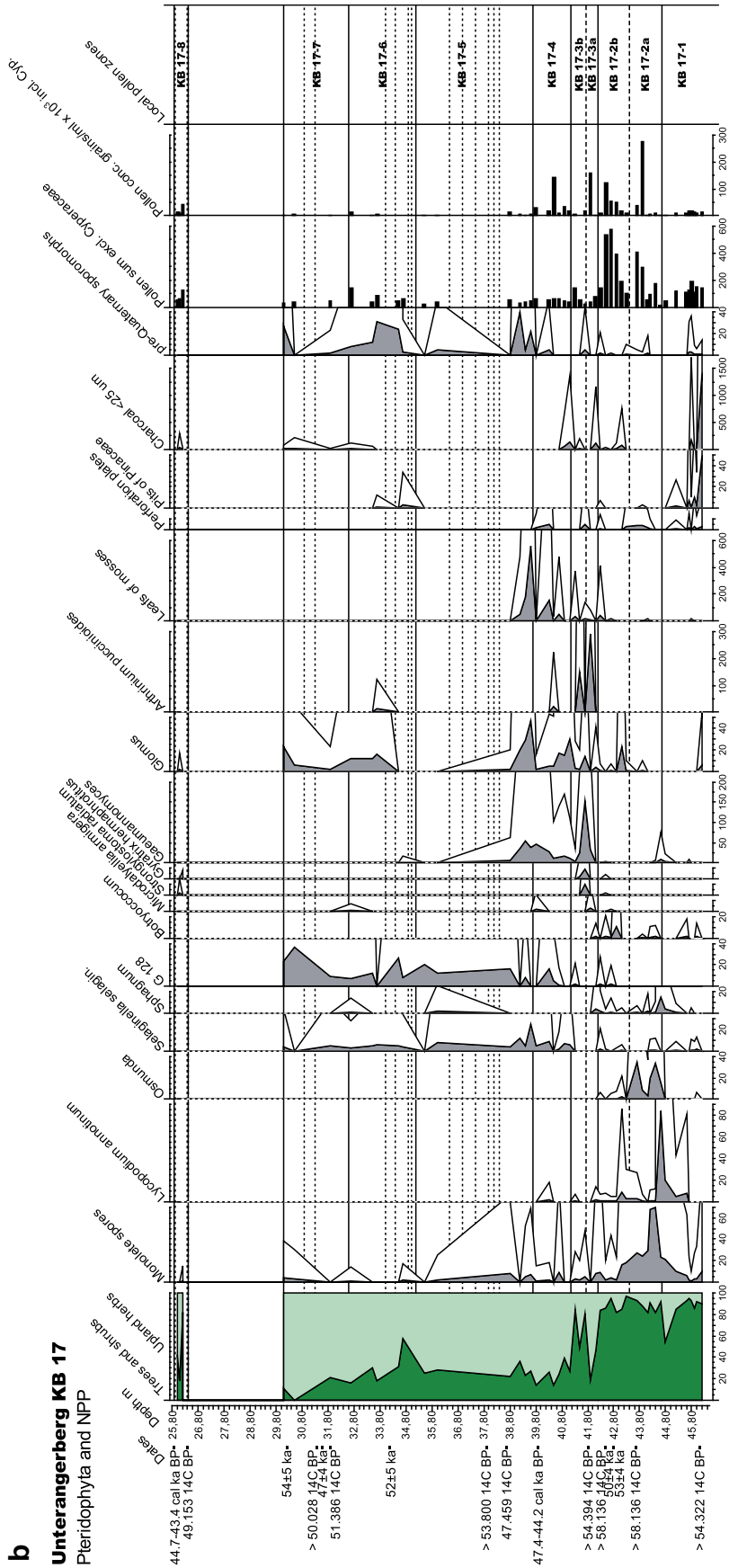

Fig. 9. (*continued*).

between 4 and 40%. The *Picea*-peak (at 45.6 m), along with some thermophilous taxa (*Quercus*, *Ulmus*, *Tilia*) could be the result of redeposition. A small *Betula*-peak at the end of this zone is accompanied by *Fraxinus*, *Acer*, *Corylus* and *Fagus*.

4.4.5.2. LPZ KB 17-2 (44.65–42.20 m): Picea–Alnus-forest with Osmunda. This pollen zone is dominated by *Picea*, with percentages of up to ~70%. The zone can be divided into two subzones: in LPZ KB 17-2a (44.65–43.40 m) *Picea* (50–60%) is accompanied by *Alnus* (up to ~15%) and a low presence of thermophilous trees (*Quercus*, *Ulmus*, *Tilia* and *Corlylus*). The numerous scalariform perforation plates indicate the presence of decomposed *Alnus*-wood. *Pinus* values remain low throughout this entire zone and range between ~15 and 35%. The values of monolete spores and of *Lycopodium annotinum* (44.60 m) are very high in this phase, and there is a high presence of *Osmunda* with up to 35% of the total pollen sum. In LPZ KB 17-2b (43.40–42.20 m), *Alnus* and *Osmunda* retreat, while *Picea* keeps expanding. This is also expressed by an increasing number of stomata findings. While the conditions for *Picea* growth seem to improve, the more thermophilous trees disappear.

4.4.5.3. LPZ KB 17-3 (42.20–41.15 m) Betula–Pinus–Picea zone with Cyperaceae. The pollen presence in these sediments is very low, caused by a very high density of indestructible organic remains. The onset of the subzone KB 17-3a (42.20–41.80 m) shows a dramatic drop in tree pollen from ~80 to 5% within ~20 cm of sediment, mainly caused by the rapid decline of *Picea*. At the same time, Cyperaceae and Poaceae values reach >80%. Herbs increase in species number and percentage. *Arthrinium puccinioides*, a saprophyte on different species of Cyperaceae and Poaceae (Scheuer, 1996), underlines the importance of a vegetation cover rich in sedges and grasses. In subzone KB 17-3b (41.80–41.15 m) the open land vegetation is replaced first by a simultaneous expansion of *Betula* and *Pinus,* followed by a strong increase of *Picea.* This sequence may reflect a short re-expansion of forest vegetation.

4.4.5.4. LPZ KB 17-4 (41.15–39.7 m): Cyperaceae zone with mosses. With exception of willow (*Salix),* trees seem to have disappeared during this zone. The NAP is dominated by Cyperaceae and Poaceae, accompanied by a variety of different herb types, by *Selaginella selaginoides*, *Gaeumannomyces*, moss leafs and a high presence of *Glomus* and pre-Quaternary sporomorphs.

4.4.5.5. LPZ KB 17-5 (39.7–35.2 m): Cyperaceae zone with very low pollen sums. This zone is situated in debris-flow deposits. Very low pollen concentrations and a reduced diversity of the pollen spectrum were found in all samples analysed from this zone.

4.4.5.6. LPZ KB 17-6 (35.2–32.6 m): Betula–Pinus–Picea zone. The pollen concentration remains very low, but the pollen sums increase due to a higher pollen density. There are representatives of a modest shrub flora, including *Ephedra*, *Hippophaë*, *Juniperus* and *Salix*, as well as some low values of *Betula*, *Pinus*, *Picea* and *Alnus*. However, these might be the result of reworking of older sediment, as suggested by individual findings of *Quercus*, *Fraxinus*, *Corylus* and *Fagus* pollen. Reworking is also indicated by an increased number of pre-Quaternary sporomorphs.

4.4.5.7. LPZ KB 17-7 (35.6–30.1 m): Herb-zone. In this zone the trees and shrubs retreat in favour of grasses (Poaceae) and heliophilous herbs such as *Artemisia*, *Helianthemum* and *Thalictrum*. Reworking of sediment continues, as indicated by pre-Quaternary sporomorphes which, however, is less abundant than in the previous zone.

4.4.5.8. LPZ KB 17-8 (26.42–25.95 m): Pinus–Picea zone with Apiaceae. After a gap between 30.0 and 26.42 m due to core loss, this uppermost zone occurs below the erosional gap beneath the overlying gravel. The sediment is peat, with both moderate pollen concentrations and pollen sums. Arboreal pollen values range from ~10 to 40%, with *Pinus* and *Picea* as dominating species. The herbal flora is rich, with remarkably high values of Apiaceae (carrot family).

4.4.6. Interpretation of the pollen data

Large portions of the cores A-KB 13/98, A-KB 14/98 and A-KB 15/98 contain no or only very few pollen grains. In core A-KB 13/98, three of five samples are pollen-free whilst the other two show extremely low pollen concentrations. The highest tree pollen percentages are due to *Pinus*, with 8% (51.51 m) and 10% (46.05 m). Among the herbs, grasses (Poaceae) and sedges (Cyperaceae) are dominant. Altogether, the results from core A-KB 13/98 indicate a relatively cool interstadial climate, and an open unforested landscape.

Local pollen zones with low concentrations (LPZ KB 15-3; KB 16-5, 16-6; KB 17-5, 17-6, 17-7) are characterised by arboreal pollen percentages not exceeding 40% and low diversity of herb species indicating open vegetation with scattered individual trees or small tree stands. The presence of some pollen grains of thermophilous trees such as *Quercus*, *Fagus*, *Fraxinus*, and *Corylus* (see LPZ KB 17-6), together with an increased frequency of pre-Quaternary sporomorphs are indicators of re-worked older sediment (Pini et al. 2009; Dehnert et al., 2012).

A nearly complete interstadial is preserved in the lower part of core A-KB 17/98, i.e. LPZ KB17-1 and KB 17-2. It starts with a reforestation phase (LPZ KB 17-1) with *Pinus* sp. *P. cembra*, *Betula* and *Salix*, but reworked pollen grains (*Quercus*, *Ulmus*, *Tilia*, etc. as well as *Lycopodium annotinum*) are also present. The presence of *P. cembra* is remarkable, because today *P. cembra* grows near the timberline, especially in the Central Alps. In older periods this species is recorded as a pioneer tree at the transition from stadials or glacials to interstadials or late glacial environments (e.g. Drescher-Schneider, 2000; Wick, 2006; Kaltenrieder et al., 2006) indicating rather continental climatic conditions (Körner, 2003).

In this pollen record the forest succession continues with a rather weak birch (*Betula)* development (end of LPZ KB 17-1) and the rapid spreading of spruce (*Picea)* at the transition from LPZ KB 17-1 to LPZ KB 17-2a. This rise is accompanied by thermophilous taxa like *Quercus*, *Ulmus*, *Tilia*, *Osmunda* and *Alnus*, indicating that the warmest phase of the interstadial was during its early part. The sediment in this period is a fine grained gyttja. Later, the sediment changes towards a calcareous gyttja (including oogonia of Characeae). At the same time, warm-demanding species decrease or totally disappear in LPZ KB 17-2b and the forest vegetation is almost entirely dominated by spruce and some pine. The presence of *Lycopodium annotinum* spores in both subzones indicates humid as well as acidic coniferous forest habitats during the interstadial forest phase. The single findings of *Fagus* are interpreted as long-term transport.

The presence of *Osmunda* in this pollen profile, especially in the interstadial as reflected in LPZ KB 17-2a, is remarkable, as it offers chronological constraints. Late Pleistocene findings of *Osmunda* spores are also reported from the northern alpine foreland at Mondsee (Drescher-Schneider, 2000), Samerberg (Grüger, 1979), Füramoos (Müller et al., 2003), and Niederweningen (Anselmetti et al., 2010; Dehnert et al., 2012). At these sites, a dense forest vegetation dominated by spruce and the presence of *Osmunda* as well as the absence of *Abies* characterised the climatic conditions during the second Early Würmian interstadial. A comparison of the Unterangerberg interstadial with the second Würmian

interstadial e.g. at Mondsee and Samerberg (the latter being only ~30 km away from Unterangerberg) reveals striking similarities and leads to the conclusion that the second Early Würmian interstadial is preserved in the Unterangerberg record. Müller (2000) and Müller and Sánchez Goñi (2007) correlated the second early Würmian interstadial (related to the Odderade interstadial in northern Europe) to the MIS 5a which is dated to between ~81.5 and 73 ka.

The diamictic layer in core A-KB 15/98 contains an organic-rich sediment horizon at 52.6 m depth (LPZ KB 15-1) which has a pollen assemblage nearly identical to the one found in PZ 17-2a. Together with the observation that the samples above and below this horizon are pollen-free this indicates further that the material is likely reworked.

The sediment of LPZ KB 17-3a is rich in organic matter near the basis (LPZ KB 17-3 and 4), with seeds (undetermined) together with a large amount of charcoal particles. The pollen content of this lignite layer reflects the onset of a stadial/interstadial sequence with open vegetation, dominated by grasses and sedges infected with the fungal species *Arthrinium puccinioides* and *Gaeumannomyces*. In the overlying, massive and organic-bearing lake sediment layer, the succeeding development to a scattered birch-pine forest and finally a spruce forest (LPZ KB 17-3b) is represented. The following organic-rich section (A-KB 17/98, 41–39.8 m) is the lower portion of a diamict layer classified as mudflow deposit. It contains pollen from possibly cold stadial climatic conditions, with grassland and weak shrub vegetation with willow (LPZ KB 17-4). The interstadial in KB 17-3b might be correlated with LPZ KB 16-1. The upper part of this diamict layer (up to 35 m core depth) (LPZ KB 17-5), is almost free of pollen, with a spectrum indicating stadial conditions. The top of the layer (35.2–24.0 m) has again a very low pollen concentration. However, the pollen spectrum here, however, seems to reflect slightly improved environmental conditions. Due to the fact that the lithology of this diamict is rather homogenous and only the organic macro- and micro-remains are present especially near the basis, allow this sediment to be related to a debris-flow. It is the presence of macro-remains such as seeds and mosses that render a glacial origin of the deposit highly unlikely, because these remains are too fragile to be preserved in a glacial environment.

Another well-developed interstadial is identified in PZ16-3, PZ 15-2 and potentially in A-KB 14/98 (46.3 m), characterised by relatively high values of *Betula* and the presence of *Pinus cembra*. This interstadial could also be present in PZ 17-6 and A-KB 14/98 (50.2 and 46.05 m).

PZ 16-3 and PZ 15-2 are followed by zones with decreasing arboreal pollen values (PZ 16-4, PZ 15-3) indicating absence and/or very low abundance of trees and the existence of a relatively diverse herbal flora and aquatic life. While core A-KB 15/98 ends with this zone due to erosion, core A-KB 16/98 contains another pollen zone following this cool interstadial, with slightly higher arboreal pollen percentages but still a very limited herbal spectrum and some indications of pre-Quaternary elements (PZ 16-5). The interpretation of this zone is difficult as it is likely that also at least some arboreal pollen are re-deposited during cold conditions with poor vegetation cover. However, the pre-Quaternary sporomorphs increase to large numbers during the following PZ 16-6, indicating an ongoing climatic deterioration. A similar picture is given by PZ 17-7.

In core A-KB 17/98 there is a last organic-rich layer below the gravel layer which underlies the LGM till. This PZ 17-8 has again a relatively high pollen concentration, with arboreal pollen indicating scattered patches of coniferous tress (*Pinus* and *Picea*). The rich herbal flora points to climatic conditions that are found at the present-day timberline.

5. Discussion

The drill cores provide unique insights into the sedimentation history of the terrace of Unterangerberg and preserve a rare inner-alpine record of the Upper Pleistocene (Figs. 10a, b and 11). The paleo-topography is strikingly different from the modern landscape of this terrace, with up to ca 200 m of Pleistocene sediments deposited in a depression. Lithological, palynological and chronostratigraphical data provide a means to correlate between individual cores along a NE-SW transect (Fig. 10a).

5.1. Unit I: oldest glacial till

Oligocene conglomerates and marls form the base of the Quaternary in the study area. In the southwest of the terrace where the bedrock is at its highest elevation (~630 m a.s.l.), it is directly overlain by LGM till (e.g. core A-KB 18/98). Among the cores penetrating pre-LGM lacustrine sequences only A-KB 17/98 reached the base of the Pleistocene fill, with a thick till at the base. Given the Late Pleistocene age of the overlying deposits, this till is possibly from the penultimate (Riss) glaciation. This glaciation was slightly more extensive than the LGM in the Eastern Alps (e.g. Ehlers and Gibbard, 2004; Doppler et al., 2011; van Husen and Reitner, 2011) and likely contributed to the sculpturing of the paleo-topography at Unterangerberg which then formed the framework for all subsequent sedimentation processes.

5.2. Unit II: Early Würmian lake phase 1 (early MIS 5d)

The oldest fine-grained sediments are found at the base of P-KB 01/06 and in the lower parts of cores A-KB 14/98 and A-KB 15/98. The luminescence ages indicate a latest Eemian (MIS 5e) to earliest last glacial (MIS 5d) deposition, however, the high sedimentation rates and the absence of organic remains argue for a MIS 5d deposition. After the demise of the Eemian this first stadial was a phase of dramatic climate deterioration leading to collapse of forests in the northern alpine foreland (Grüger, 1979; Drescher-Schneider, 2000; Müller, 2000; Müller et al., 2003) and the onset of loess deposition (Zöller et al., 1994; Thiel et al., 2011). In the Western Alps there is evidence for a pronounced glacier advance into lowland altitudes at that time (e.g. Preusser et al., 2003), while in the Eastern Alps only strong fluvial aggradation is documented (Reitner, 2005; Reitner et al., 2010).

5.3. Unit III: Butterbichl paleo-landslide (early MIS 5d)

Core P-KB 01/06 comprises the complete stratigraphy of the landslide deposits as well as their lacustrine base and the overlying LGM till. The latter offers a maximum age of the event which has been known since the first investigations of Penck and Brückner (1909). The two luminescence ages at the bottom of the core yield values of ~114 and 113 ka which – considering the age uncertainties – again indicates MIS 5e or MIS 5d deposition. As for unit II, deposition under stadial (i.e. MIS 5d) conditions is presumed, although part of the lacustrine sequence may have been eroded during the emplacement of the landslide (Gruber et al., 2009).

The MIS 5d luminescence ages are in fairly good agreement with data obtained from Entrische Kirche and Spannagel caves, both within 40–50 km of Unterangerberg. At these sites, U-series dated speleothems show a major drop in $\delta^{18}O$ values at ~119–117 ka reflecting strong cooling at the end of the Eemian interglacial (Spötl et al., 2006; Meyer et al., 2008). The Butterbichl landslide with its estimated total volume of ~300 Mio m^3 is one of the largest mass movements known in the Eastern Alps (Gruber et al.,

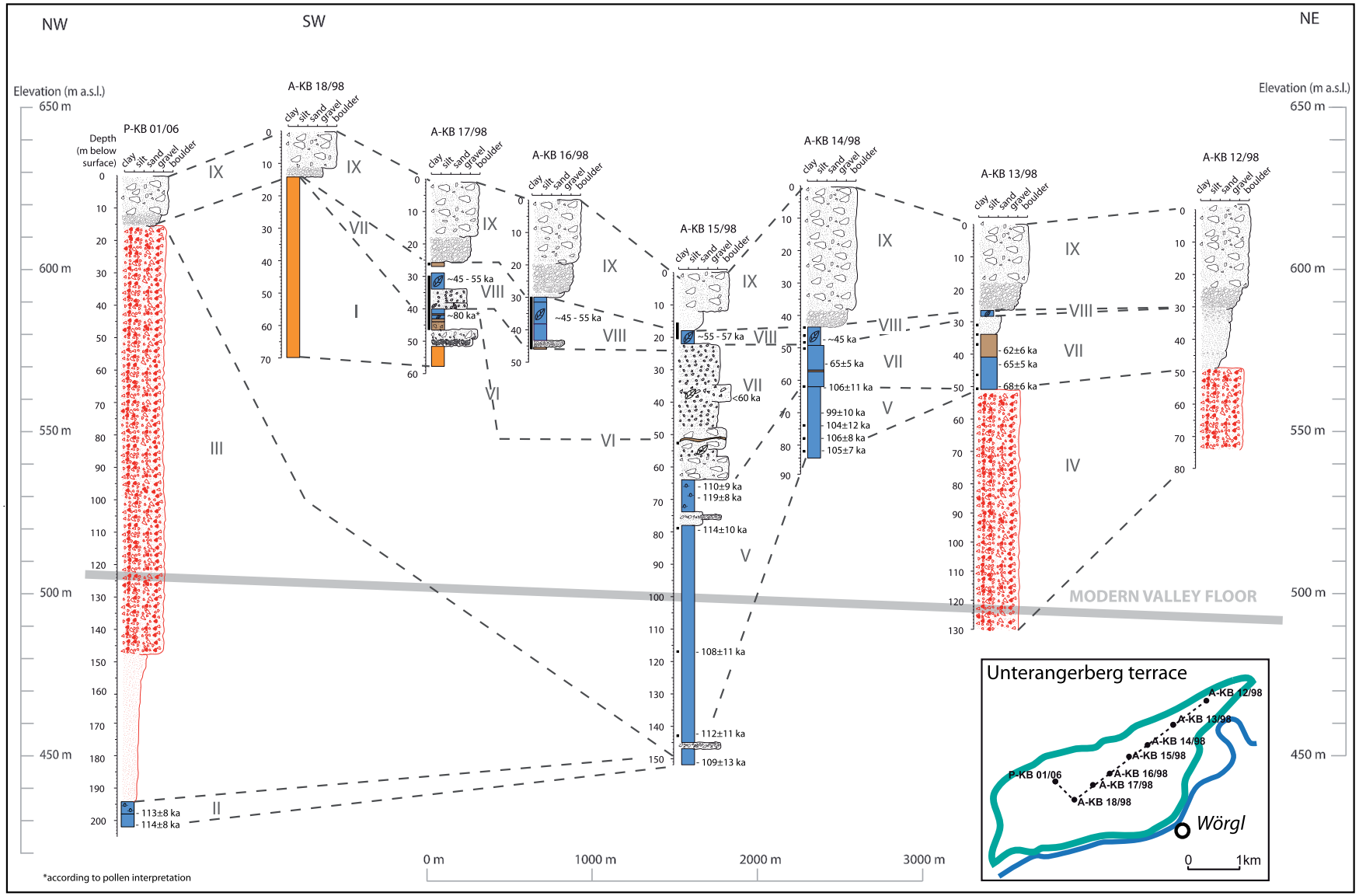

Fig. 10. a: Schematic overview of cores along a NE–SW–NW profile across the Unterangerberg terrace, with core lithologies, absolute ages (combined radiocarbon and luminescence data), pollen samples (black bars right to core depth scale), and chronostratigraphical units (I to IX, see text for details). b: Overview of core lithologies and comparison of radiocarbon (cal ka BP, black numbers) and luminescence (ka, red dots and red numbers) dating results for Unterangerberg cores A-KB 14/98, A-KB 15/98, A-KB 16/98 and A-KB 17/98. (For interpretation of the references to color in this figure legend, the reader is referred to the web version of this article.)

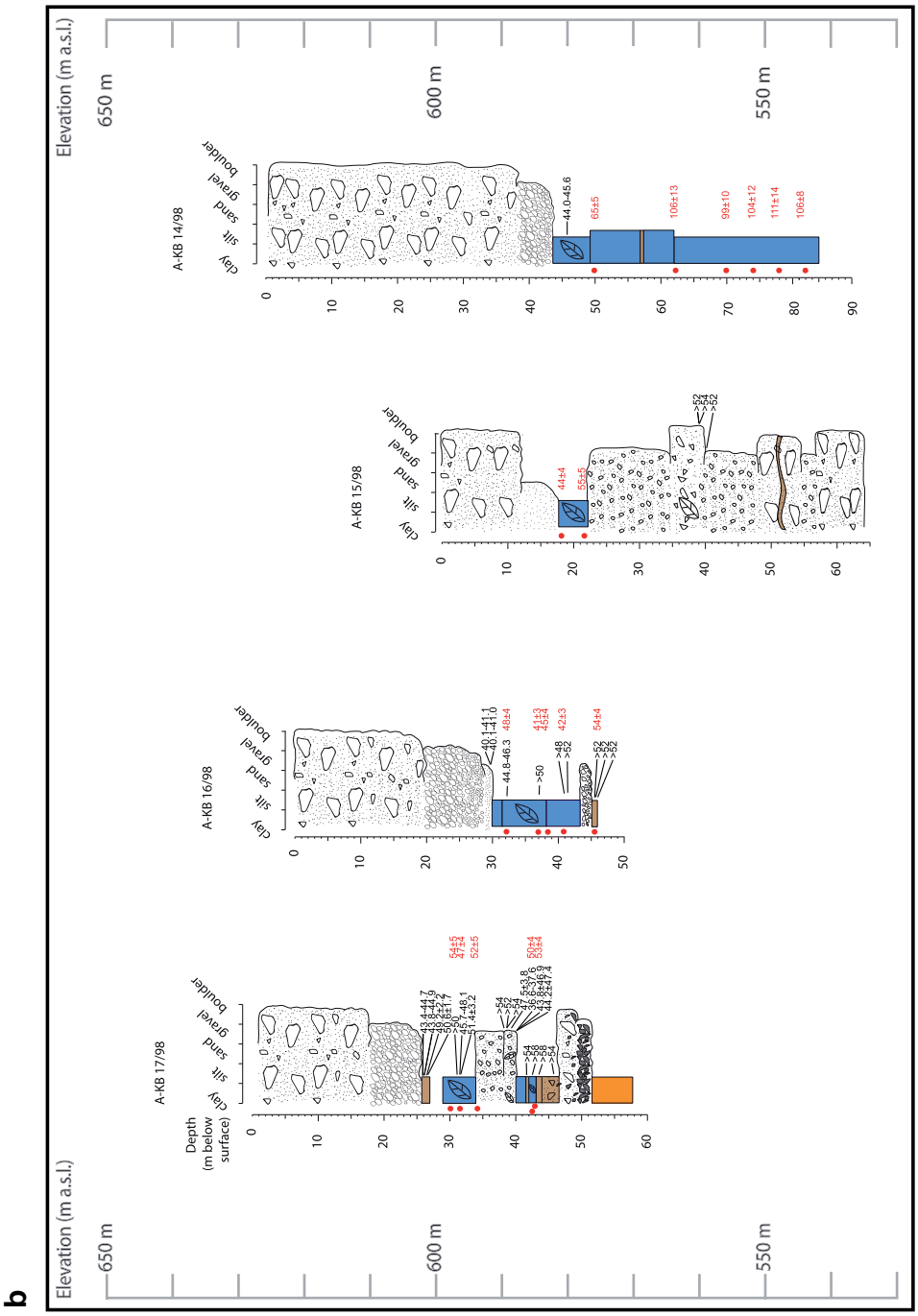

Fig. 10. (*continued*).

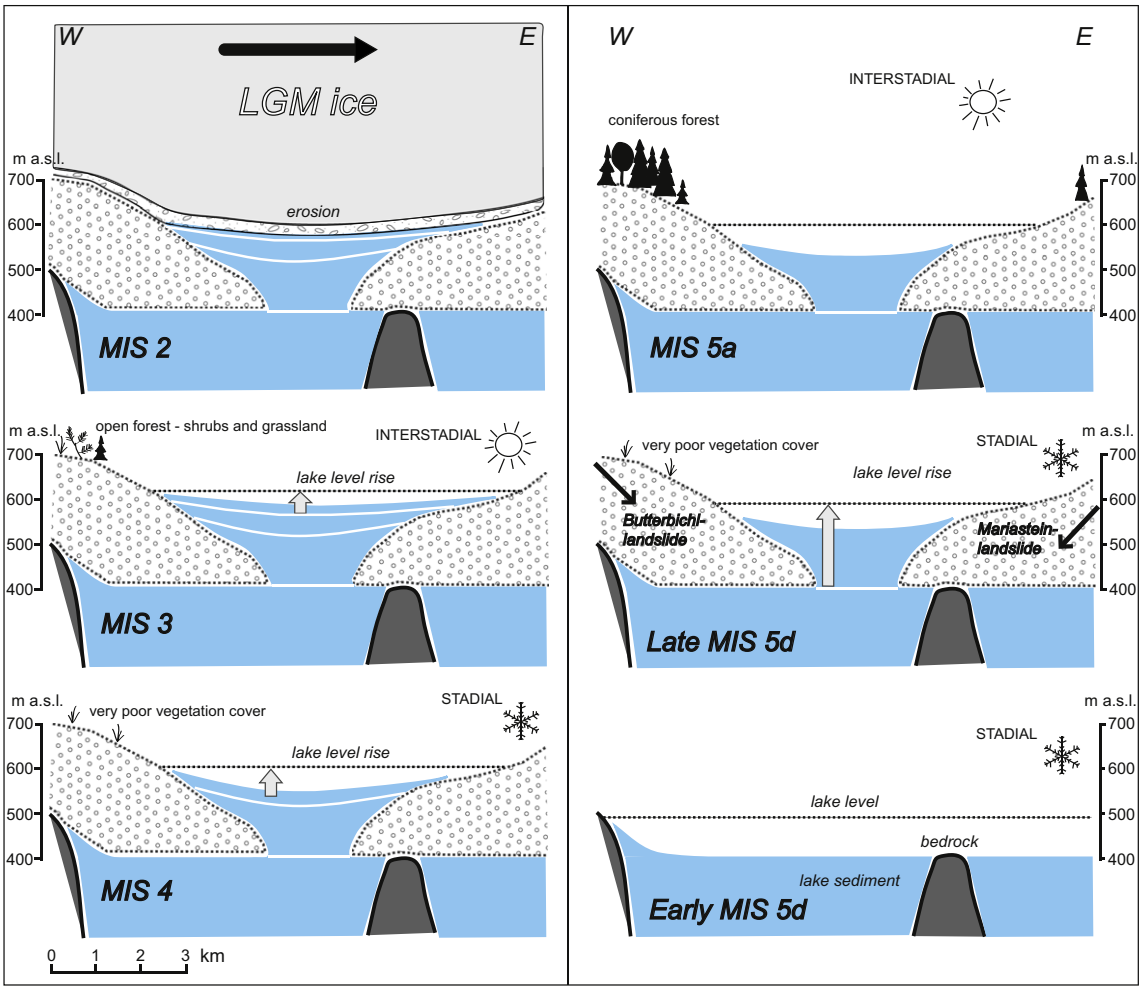

Fig. 11. Schematic overview of lacustrine sedimentation and local vegetation history at Unterangerberg between MIS 5d and 2 as reconstructed from drillcores. Major sedimentary gaps are present for MIS 5b-c and during the late MIS 3.

2009). Its deposition at the onset of the last glacial period could have been climatically triggered, although earthquakes should also be considered as a cause given the neotectonic activity of the nearby Inntal Fault.

5.4. Unit IV: Mariastein paleo-landslide (Early MIS 5d)

The second landslide at Unterangerberg occurred only ~7 km W of the Butterbichl, near the village of Mariastein. First mentioned by Penck and Brückner (1909), this event is less well studied than the Butterbichl landslide (Ampferer, 1922; Heissel, 1951). The reconstruction of the escarpment leads to the conclusion that this event was of a similar dimension as the Butterbichl landslide (Gruber, 2008). Unfortunately, none of the cores penetrated the landslide cataclasite. Field evidence, however, indicates deposition of the Mariastein landslide onto Pleistocene fine grain lacustrine sediments (Heissel, 1951; Gruber, 2008). Lake sediments were then deposited on top of the cataclasite (core A-KB 13/98) and dated to ~68–62 ka, i.e. MIS 4. Further, strongly weathered clasts in the upper part of the cataclasite might be relics of paleosol. In this case, the landslide event was followed by a period without sedimentation, possibly under interstadial conditions, before the area was flooded by a lake. Consequently, the MIS 4 ages should be considered as minimum ages. The strong similarities between the Butterbichl and the Mariastein landslide events point at a synchronicity of these two events (Gruber, 2008), although this cannot be verified using present chronological techniques.

5.5. Unit V: Early Würmian lake phase 2 (Late MIS 5d)

After the two landslide events lacustrine deposition continued under stadial conditions until ~100 ka (cores A-KB 14/98 and A-KB 15/98). In contrast to evidence for a lowland glacier advance in northern Switzerland at ~103 ka (Preusser et al., 2003; Preusser and Schlüchter, 2004), the character of the lake sediments at Unterangerberg argues against ice in the lower Inn valley during MIS 5d.

5.6. Unit VI: 2nd Early Würmian Interstadial (EWI) (MIS 5a)

This unit is characterised by a succession of organic-rich lacustrine layers between ~583 and 589 m a.s.l. in core A-KB 17/98, with a paleosol-peat-lake sediment-peat sequence between ~46 and 40 m depth and a till at its base attributed to MIS 6. Unit VI comprises a long forest interstadial (pollen zones 17-1 and 17-2) followed by a stadial with open vegetation (PZ 17-3). Between 44 and 40 m, changes in the organic carbon content coincide with changes in vegetation composition as shown by pollen zones 17-1 and 17-2 (Fig. 9a and b). The vegetation of this interstadial was very similar to what is known from the second Early Würmian

Interstadial, e.g. from Mondsee (Drescher-Schneider, 2000) and Samerberg (Grüger, 1979), correlated to MIS 5a and dated at ~81.5–73 ka (Müller and Sánchez Goñi, 2007). However, there are two OSL ages (core A-KB 17/98, at 42.5 and 41.8 m depth) from the lacustrine sequence of this forested interstadial at Unterangerberg indicating deposition of the sediment between ~57 and 46 ka, i.e. early MIS 3. This, however, is in conflict with the palynological account and therefore requires closer investigation: high-resolution gamma spectrometry of samples close to these two luminescence-dated samples ages, shows that age estimation due to radioactive equilibrium in the U-decay series of these two samples can be excluded (F. Preusser, pers. com. 2011). No anomalous fading of the luminescence signal was detected, as outlined in Section 1.1.2 showed. Furthermore, in order to yield a signal loss that would account for an age underestimation of ~30 ka as in this case, a rather high *g*-value of ~4.5% would be needed. We also rule out an underestimation of water content as a cause for these young ages. In order to obtain a depositional age in agreement with the palynological age, i.e. MIS 5a, an unrealistically high paleo-water content of 80–90% would be required. This, together with the facts that the respective luminescence ages are in agreement with the other luminescence data from this core and that the calibrated radiocarbon data are in general agreement with these other luminescence ages, leaves little doubt about the validity of the data. On the other hand, dated wood pieces from the two organic layers in core A-KB 17/98 (44–40 m) and the underlying possible fossil soil (A_KB 17/98, 46.1 m, see Table 3) resulted in infinite ages >~58–54 ka, indicating at a deposit prior to this time.

In fact, MIS 3 interstadials comparable in their paleovegetation to MIS 5a or 5c are completely unknown from any other alpine sites so far. For instance, studies at Gossau (Swiss northern alpine foreland) indicate mean July temperatures of ~10–13 °C (Jost-Stauffer et al., 2005; Coope, 2007) and a forest tundra vegetation with typically no more than ~20–40% arboreal pollen at ~50–45 ka (Burga, 2006; Drescher-Schneider et al., 2007; Dehnert et al., 2012). An interstadial with an open *Picea*-forest at ~45 ka is documented from the mammoth site of Niederweningen, ~40 km NW of Gossau (Drescher-Schneider et al., 2007; Hajdas et al., 2007; Preusser and Degering, 2007). The comparison of these data with those from our new work at Unterangerberg leads to the conclusion that the warm forest interstadial in this unit represents MIS 5a rather than MIS 3 as suggested by two IRSL dates. The apparent contradiction between the luminescence and the palynological data remains unsolved.

5.7. Unit VII: Early Middle Würmian (MIS 4) stadial conditions

In core A-KB 14/98 the MIS 5d clayey-silty sediments are topped by a sequence of sandy silt up to ~583 m a.s.l., with an abrupt transition at 564.47 m. In the upper part, this layer shows occasional lamination. An IRSL age of ~65 ka indicates deposition during the Early Middle Würmian (MIS 4), i.e. the sharp boundary represents a hiatus of ~40 ka. In the neighbouring core A-KB 13/98 there is a similar layer which has a base situated at the same elevation. Here, however, the lake sediment was deposited on top of the Mariastein landslide deposit and is overlain by fine sand of unknown age. The sediments from these two cores indicate a lake during MIS 4 and a strongly reduced vegetation cover as indicated by the pollen. The thick diamict layer in core A-KB 15/98 is in the upper part at the same elevation as the Early Middle Würmian lacustrine sequence. This diamict is interpreted as a debris-flow event during MIS 4, because (i) it eroded and redeposited an organic layer of the 2nd EWI, and (ii) it contains wood that is dated to >60 ka.

In summary, Unit VII recorded very poorly developed vegetation and enhanced surface processes during MIS 4. There is no evidence for a glaciation during this time.

5.8. Unit VIII: Middle Würm (MIS 3) stadial/interstadial conditions

The youngest lake phase at Unterangerberg is the best preserved one and was identified in five cores. It is also the phase of the highest lake level (slightly over 600 m a.s.l.) (see Fig. 11). On basis of the cores and the chronology, the highest and youngest point with lake sediments is situated at 604 m a.s.l. (A-KB 17/98) where the deposition of a fine grained gyttja indicates a littoral position. The deepest MIS 3 lake deposits are situated at ~578 m a.s.l. (A-KB 15/98). The sequence continues up to ~582 m a.s.l., where the sediment has roughly the same age as the above-mentioned gyttja. Regardless of the erosional impact of the following LGM glaciation which certainly removed MIS 3 sediments to some extent, a water depth of ~20 m is deduced from these observations (by comparing the elevations of the topmost lake sediments in the cores A-KB 17/98 and 15/98). Whether this represents the maximum depth of the lake at that time remains unknown. However, due to the previous sedimentary filling of the basin (two landslides, aggradation during MIS 5a) a much deeper MIS 3 lake seems highly unlikely.

Luminescence and calibrated radiocarbon ages of ~55–45 ka indicate a Middle Würm (MIS 3) age of this unit. The plant remains point to a high productivity of the lake, with abundant Characeae. Pollen data indicate open vegetation dominated by grasses and herbs during stadial conditions. Tree pollen values range between 10 and 20%, with *Pinus* and *Betula* and low values of *Picea*. Interstadials were characterised by open forests (~30–50% AP) and were dominated by *Pinus*. Although the available chronological data do not allow the unequivocal correlation of this warm phase identified in A-KB 15/98 (PZ 15-2) and A-KB 16/98 (PZ 16-2) to a particular interstadial in Greenland. GI 14, however, is the most likely candidate for this warm phase. This interstadial started 54.2 ka ago and was the longest one in MIS 3 (until 49.5 ka; Svensson et al., 2008). GI 14 is also recorded in the oxygen isotopic composition of stalagmites from Kleegruben Cave, located 55 km SW of the study area (Spötl and Mangini, 2002; Spötl et al., 2006).

Middle Würmian vegetation records are only poorly preserved in previously studied sites in the northern Alpine foreland, such as Samerberg (Grüger, 1979), Mondsee (Drescher-Schneider, 2000), Jammertal (Müller, 2000) and Füramoos (Müller et al., 2003) and none of these sites has an independent chronology. In the Swiss alpine foreland MIS 3 paleovegetation records are more common, including at Niederweningen and Gossau. At the mammoth site in Niederweningen arboreal pollen percentages of 20–40% suggest open grassland vegetation ~50–45 ka ago. Similar to Unterangerberg, the interstadial forest vegetation was characterised by *Pinus*, *Betula* and *Picea* (Drescher-Schneider et al., 2007; Hajdas et al., 2007; Preusser and Degering, 2007). Near Gossau, southeast of Zurich, a sequence of organic-rich sediments deposited on top of delta foresets contains an interstadial complex ranging from tundra to woodland (Preusser et al., 2003). While the two upper lignite layers, dated at ~48–32 ka, suggest tundra to steppe vegetation, the lower lignite layer (~50 ka) was characterised by a forest dominated by *Picea* and *Pinus* (Welten, 1982; Schlüchter et al., 1987; Preusser, 1999; Preusser et al., 2003). Fossil beetle assemblages indicate mean July temperatures of ~13 °C for the lower lignite (Jost-Stauffer et al., 2005), ca 5 °C lower than today.

5.9. Unit IX: Proglacial and glacial deposits (LGM)

Today's surface of the Unterangerberg terrace is mainly composed of glacial till of the LGM. This till overlies glaciofluvial

gravel which is attributed to strong aggradation of the Inn River as a result of progressive glacier advance from the tributaries into the main valleys. Radiocarbon ages of ~41–40 cal ka BP (A-KB 16/98; 29.8 and 29.9 m) represent a maximum age for the onset of this phase. The transition from the Middle to the Upper Würmian, i.e. from MIS 3 to 2 in the Alps, was defined at Baumkirchen, ~35 ka SW of Unterangerberg. At this location, a coarsening-up sequence of laminated silt, sand, gravel and till is exposed, with radiocarbon ages of ~31–26 cal ka BP obtained from the lacustrine silt (Fliri, 1973). At Unterangerberg, the amount of erosion of pre-LGM sediments by the advancing ice is unknown but was probably only minor on the terrace compared to the central Inn valley.

The Unterangerberg record presented in this study contributes an inner-alpine perspective to the Early to Mid Late Pleistocene palaeoclimate reconstructions in Europe. The glacial inception at ~115–105 ka at Unterangerberg coincided with a drop in oxygen isotope values in Greenland ice (Svensson et al., 2008; Wolff et al., 2010) and in stalagmites from the Alps (Spötl and Mangini, 2006; Meyer et al. 2008; Boch et al., 2011) and southern Europe (e.g. Drysdale et al., 2005, 2007). For this first Late Pleistocene stadial decreasing temperatures and precipitation sums, steep N–S vegetation gradients and a retreat of the forest line to south-central Europe (e.g. Caspers and Freund, 2001; Sánchez Goñi et al., 2005; Müller and Sánchez Goñi, 2007; Brewer et al., 2008), as well as loess deposition in Eastern European sites (e.g. Gerasimenko, 2006) are reported. During the following MIS 5 interstadials (i.e. MIS 5c and MIS 5a) forests re-established throughout Europe, however, under increasingly continental climatic conditions (e.g. Emontspohl, 1995; Caspers and Freund, 2001; Kühl et al., 2007).

MIS 4 (~70–60 ka) was a generally cold period in Europe, with forests only remaining in the southern and south-eastern margin of the continent (Fletcher et al., 2010) and extensive loess accumulation under permafrost conditions (Frechen et al., 2003; Rousseau et al., 2007). Evidence for a major Alpine lowland glaciation is emerging in the Western Alps (Preusser, 2004; Preusser and Schlüchter, 2004; Preusser et al., 2007) but is absent in the Eastern Alps. At Unterangerberg, a lake was present during the time period ~70–60 ka, recording a sparsely vegetated environment characterised by enhanced down-wasting processes.

During MIS 3, changing stadial/interstadial conditions continued to dominate the climate in Europe. These large swings are reflected in synchronous changes of the stable isotope compositions in Greenland (Svensson et al., 2008) and – as documented for the prominent interstadial 14 – in the Alps (Spötl and Mangini, 2006). D/O-cycles had a drastic impact on the European vegetation (Vandenberghe et al., 2004; Fletcher et al., 2010; Harrison and Sánchez Goñi, 2010; Van Meerbeeck et al., 2011) with strongly reduced vegetation and extensive loess deposition under stadial conditions (Fletcher et al., 2010). Interstadials gave rise to grassland, shrub tundra and extensive forest-tundra in northern and NW Europe, open boreal forest in W Europe and north of the Alps and open temperate deciduous forests in southern Europe (Caspers and Freund, 2001; Tzedakis 2005; Fletcher et al., 2010). MIS 3 interstadial temperature reconstructions indicate very cold winters and relatively warm summers, with reconstructed mean temperatures of the warmest month ranging between ~8 and 16 °C (e.g. Huijzer and Vandenberghe, 1998; Kasse et al., 1998; Jost-Stauffer et al., 2005; Coope, 2007; Engels et al., 2008a). Some studies, however, reported present-day Early MIS 3 summer temperatures e.g. from NW Europe (Coope, 2002) and north Scandinavia (Engels et al., 2008b; Helmens and Engels, 2010; Helmens et al., 2012). At Unterangerberg, MIS 3 (~55–45 ka) interstadial conditions were characterised by a mix of open conifer forests and grassland, similar to the vegetation at the present-day alpine timberline.

6. Conclusions

The investigations carried out at the terrace of Unterangerberg result in the first detailed Late Pleistocene record of sedimentation and paleoenvironments inside the Alps for the time period ~118–40 ka, with a hiatus between ~100 and 80 ka. Three lake phases could be identified, reflecting both stadial and interstadial climatic and environmental conditions throughout the early and middle Würmian. The warmest interstadial found in our record was characterized by conifer forests and based on pollen data is correlated with the second early Würmian Interstadial (MIS 5a). Interstadials of the first half of the Middle Würmian (~55–45 ka) are chronometrically well constrained, with open forests and mixed grassland vegetation. Stadials were generally characterised by high sedimentation rates, low organic deposition and cold-adapted open (tundra) vegetation. For the entire period represented by these sediments there is no evidence of ice in the lower Inn valley, consistent with the results of a previous study from nearby valleys (Reitner, 2005).

Acknowledgements

This study was made possible by core material provided by the Brenner Railway Company (BEG) and funding by FWF (grant P208580 to C. Spötl). Christoph Sedlacek, Manfred Köhler (both BEG) and Martin Weber are thanked for logistic support, Christoph Prager for one radiocarbon date, and Frank Preusser for providing high-resolution gamma spectrometry measurements. H. Mayrhofer, leader of the department Systematic and Ecology of Institute of Plant Science of Karl-Franzens-University of Graz, is thanked for supporting the preparation of the pollen samples in his laboratories.

Appendix A. Supplementary material

Supplementary material related to this article can be found at http://dx.doi.org/10.1016/j.quascirev.2013.02.008.

References

Adamiec, G., Aitken, M., 1998. Dose-rate conversion factors: update. Ancient TL 16, 37–50.
Aitken, M.J., 1998. An Introduction to Optical Dating. Oxford University Press, Oxford.
Ampferer, O., Ohnesorge, T., 1909. Über exotische Gerölle in der Gosau und verwandte Ablagerungen in den tirolischen Nordalpen. Jahrbuch der Geologischen Reichsanstalt 59, 288–332.
Ampferer, O., 1922. Zur Geologie des Unterinntaler Tertiärs. Jahrbuch der Geologischen Bundesanstalt 172, 105–150.
Anselmetti, F.S., Drescher-Schneider, R., Furrer, H., Graf, H.R., Lowick, S.E., Preusser, F., Riedi, M.A., 2010. A ~180.000 years sedimentation history of a perialpine overdeepened glacial trough (Wehntal, N-Switzerland). Swiss Journal of Geosciences 103, 345–361.
Auclair, M., Lamothe, M., Huot, S., 2003. Measurement of anomalous fading for feldspar IRSL using SAR. Radiation Measurements 37, 487–492.
Beniston, M., 2003. Climatic change in mountain regions: a review of possible impacts. Climatic Change 59, 5–31.
Benn, D.I., Evans, D.J.A., 1998. Glaciers and Glaciation. Arnold, London.
Berglund, B.E., Ralska-Jasiewiczowa, M., 1986. 22. Pollen analysis and pollen diagrams. In: Berglund, B.E., Ralska-Jasiewiczowa, M. (Eds.), Handbook of the Holocene Palaeoecology and Palaeohydrology. John Wiley & Sons, Chichester.
Beug, H.-J., 2004. Leitfaden der Pollenbestimmung für Mitteleuropa und angrenzende Gebiete. Pfeil, Munich.
Boch, R., Cheng, H., Spötl, C., Edwards, R.L., Wang, X., Häuselmann, P., 2011. NALPS: a precisely dated European climate record 120–60 ka. Climate of the Past 7, 1247–1259.
Brewer, S., Guiot, J., Sánchez-Goñi, M.F., Klotz, S., 2008. The climate in Europe during the Eemian: a multi-method approach using pollen data. Quaternary Science Reviews 27, 2303–2315.
Burga, C., 2006. Zum Mittelwürm des Zürcher Oberlandes am Beispiel des Schieferkohle-Profils von Gossau (Kanton Zürich). Vierteljahresschrift der Naturforschenden Gesellschaft in Zürich 151, 91–100.

Caspers, G., Freund, H., 2001. Vegetation and climate in the Early- and Pleni-Weichselian in northern central Europe. Journal of Quaternary Science 16, 31–48.
Chaline, J., Jerz, H., 1984. Arbeitsergebnisse der Subkommission für Europäische Quartärstratigraphie. Stratotypen des Würm-Glazials. Eiszeitalter und Gegenwart 35, 185–206.
Coope, G.R., 2002. Changes in the thermal climate on north-western Europe during marine isotope stage 3, estimated from fossil beetle assemblages. Quaternary Research 57, 401–408.
Coope, G.R., 2007. Coleoptera from the 2003 excavations of the mammoth skeleton at Niederweningen, Switzerland. Quaternary International 164-165, 130–138.
Cushing, E.J., 1964. Application of the code of stratigraphic nomenclature to pollen stratigraphy. In: Berglund, B.E., Ralska-Jasiewiczowa, M. (Eds.), 1986, Handbook of the Holocene Palaeoecology and Palaeohydrology. John Wiley & Sons, Chichester.
Dansgaard, W., Johnsen, S.J., Clausen, H.B., Dahl-Jensen, D., Gundestrup, N.S., Hammer, C.U., Hvidberg, C.S., Steffensen, J.P., Sveinbjörnsdottir, A.E., Jouzel, J., Bond, G., 1993. Evidence for general instability of past climate from a 250-kyr ice-core record. Nature 364, 218–220.
Dehnert, A., Lowick, S., Preusser, F., Anselmetti, F., Drescher-Schneider, R., Graf, H.R., Heller, F., Horstmeyer, H., Kemna, H.A., Nowaczyk, N.R., Züger, A., Furrer, H., 2012. Evolution of an overdeepened trough in the northern Alpine Foreland at Niederweningen, Switzerland. Quaternary Science Reviews 34, 127–145. http://dx.doi.org/10.1016/.quascirev.2011.12.015.
Doppler, G., Kroemer, E., Rögner, K., Wallner, J., Jerz, H., Grottenthaler, W., 2011. Quaternary Stratigraphy of Southern Bavaria. Quaternary Science Journal 60, 329–365.
Drescher-Schneider, R., 2000. Die Vegetations- und Klimaentwicklung im Riss/Würm-Inter-Glazial und im Früh- und Mittelwürm in der Umgebung von Mondsee. Ergebnisse der pollenanalytischen Untersuchungen. In: van Husen, D. (Ed.), Klimaentwicklung im Riss/Würm Interglazial (Eem) und Frühwürm (Sauerstoffisotopenstufe 6-3) in den Ostalpen. Mitteilungen der Kommission für Quartärforschung der Österreichischen Akademie der Wissenschaften, vol. 12, pp. 39–92.
Drescher-Schneider, R., Jaquat, C., Schoch, W., 2007. Botanical investigations at the mammoth site of Niederweningen (Kanton Zürich), Switzerland. Quaternary International 164/165, 113–129.
Drysdale, R.N., Zanchetta, G., Hellstrom, J.C., Fallick, A.E., Zhao, J., 2005. Stalagmite evidence for the onset of the last Interglacial in southern Europe at 129 ± 1 ka. Geophysical Research Letters 32. http://dx.doi.org/10.1029/2005GL024658.
Drysdale, R.N., Zanchetta, G., Hellstrom, J.C., Fallick, A.E., McDonald, J., Cartwright, I., 2007. Stalagmite evidence for the precise timing of North Atlantic cold events during the early last glacial. Geology 35, 77–85.
Ehlers, J., Gibbard, P.L. (Eds.), 2004. Quaternary Glaciations-Extent and Chronology. Part I: Europe. Elsevier, Amsterdam.
Emontspohl, A.-F., 1995. The northwest European vegetation at the beginning of the Weichselian glacial (Brørup and Odderade interstadials)-new data for northern France. Review of Palaeobotany and Palynology 85, 231–242.
Engels, S., Bohncke, S.J.P., Bos, J.J.A., Heiri, O., Vandenberghe, J., Wallinga, J., 2008a. Environmental inferences and chironomid-based temperature reconstructions from fragmentary records of the Weichselian Early Glacial and Pleniglacial period in the Niederlausitz area (eastern Germany). Palaeogeography, Palaeoclimatology, Palaeoecology 260, 405–416.
Engels, S., Bohncke, S.J.P., Bos, J.J.A., Brooks, S.J., Heiri, O., Helmens, K.F., 2008b. Chironomid-based palaeotemperature estimates for northeast Finland during Oxygen Isotope Stage 3. Journal of Paleolimnology 40, 49–61.
Fletcher, W.J., Goñi, Sánchez, Allen, J.R.M., Cheddadi, R., Combourieu-Nebout, N., Huntley, B., Lawson, I., Londeix, L., Magri, D., Margari, V., Müller, U.C., Naughton, F., Novenko, E., Roucoux, K., Tzedakis, P.C., 2010. Millennial-scale variability during the last glacial in vegetation records from Europe. Quaternary Science Reviews 29, 2839–2864.
Fliri, F., 1973. Beiträge zur Geschichte der alpinen Würmvereisung: Forschungen am Bänderton von Baumkirchen (Inntal, Nordtirol). Zeitschrift für Geomorphologie N. F. Supplement 16, 1–14.
Frechen, M., Schweitzer, M., Zander, A., 1996. Improvements in sample preparation fort the fine grain technique. Ancient TL 14, 15–17.
Frechen, M., Oches, E.A., Kohlfeld, K.E., 2003. Loess in Europe-mass accumulation rates during the Last Glacial Period. Quaternary Science Reviews 22, 1835–1857.
Gerasimenko, N., 2006. Upper Pleistocene loess-palaeosol and vegetational successions in the Middle Dnieper Area, Ukraine. Quaternary International 149, 55–66.
Gruber, A., 2008. Bericht 2005–2008 über geologische, strukturgeologische und insbesondere quartärgeologischen Aufnahmen auf Blatt UTM 3213 Kufstein. Jahrbuch der Geologischen Bundesanstalt 149, 550–564.
Gruber, A., Strauhal, T., Prager, C., Reitner, J.M., Brandner, R., Zangerl, C., 2009. Die "Butterbichl-Gleitmasse" – eine große fossile Massenbewegung am Südrand der Nördlichen Kalkalpen (Tirol, Österreich). Swiss Bulletin for Applied Geology 14, 103–134.
Grüger, E., 1979. Spätriß, Riß/Würm und Frühwürm am Samerberg in Oberbayern – ein vegetationsgeschichtlicher Beitrag zur Gliederung des Jungpleistozäns. Geologica Bavarica 80, 5–64.
Haas, J.N., 1995. Neorhabdocoela oocytes – palaeoecological indicators found in pollen preparations from Holcene freshwater lake sediments. Review of Palaeobotany and Palynology 91, 371–382.
Haesaerts, P., Damblon, F., Bachner, M., Trnka, G., 1996. Revised stratigraphy and chronology of the Willendorf II sequence, Lower Austria. Archaeologia Austriaca 80, 25–42.
Hajdas, I., Bonani, G., Furrer, H., Mäder, A., Schoch, W., 2007. Radiocarbon chronology of the mammoth site at Niederweningen, Switzerland: results from dating bones, teeth, wood, and peat. Quaternary International 164/165, 98–105.
Harrison, S.P., Sánchez Goñi, M.F., 2010. Global patterns of vegetation response to millennial-scale variability and rapid climate change during the last glacial period. Quaternary Science Reviews 29, 2957–2980.
Helmens, K.F., Engels, S., 2010. Ice-free conditions in eastern Fennoscandia during early Marine Isotope Stage 3: lacustrine records. Boreas 39, 399–409.
Helmens, K., Väliranta, M., Engels, S., Shala, S., 2012. Large shifts in vegetation and climate during the Early Weichselian (MIS 5d-c) inferred from multi-proxy evidence at Sokli (northern Finland). Quaternary Science Reviews 41, 22–38.
Heissel, W., 1951. Beiträge zur Tertiärstratigraphie und Quartärgeologie des Unterinntales. Jahrbuch der Geologischen Bundesanstalt 94, 207–221.
Heissel, W., 1955. Zur Geologie des Unterinntaler Tertiärgebietes. Mitteilungen der Österreichichen Geologischen Gesellschaft 48, 49–70.
Huber, U., Bugmann, H., Reasoner, M., 2005. Global Change and Mountain Regions. An Overview of Current Knowledge. Advances in Global Change Research. Springer, Dordrecht.
Huijzer, B., Vandenberghe, J., 1998. Climatic reconstruction of the Weichselian Pleniglacial in northwestern and Central Europe. Journal of Quaternary Science 13, 391–417.
van Husen, D., 2004. Quaternary glaciations in Austria. In: Ehlers, J., Gibbard, P.L. (Eds.), Quaternary Glaciations: Extent and Chronology Part I: Europe. Elsevier, London, pp. 1–13.
van Husen, D., Reitner, J.M., 2011. An outline of the Quaternary stratigraphy of Austria. Quaternary Science Journal 60, 366–387.
Ivy-Ochs, S., Kerschner, H., Reuther, A., Preusser, F., Heine, F., Maisch, M., Kubik, P.W., Schlüchter, C., 2008. Chronology of the last glacial cycle in the European Alps. Journal of Quaternary Science 23, 559–573.
Joerin, U.E., Nicolussi, K., Fischer, A., Stocker, T.F., Schlüchter, C., 2008. Holocene optimum events inferred from subglacial sediments at Tschierva glacier, eastern Swiss Alps. Quaternary Science Reviews 27, 337–350.
Jost-Stauffer, M., Coope, G.R., Schlüchter, C., 2005. Environmental and climatic reconstructions during Marine Oxygen Isotope Stage 3 from Gossau, Swiss Midlands, based on coleopteran assemblages. Boreas 34, 53–60.
Kaltenrieder, P., Ammann, B., Ravazzi, C., Tinner, W., 2006. Last glacial times at Lago di Costa (AP2): long-term forest dynamics during the last 26,000 years at Colli Euganei (near Padova, Italy). XXX. International Moor-Excursion 2006, Northern and Central Italy, 16.9–24.9.2006, Excursion Guide: pp. 64–66.
Kasse, C., Huijzer, A.S., Krzyszkowski, D., Bohncke, S.J.P., Coope, G.R., 1998. Weichselian Late Pleniglacial and Late-Glacial depositional environment, Coleoptera and periglacial climate records from central Poland (Belchatów). Journal of Quaternary Science 13, 455–469.
Klasen, N., Fiebig, M., Preusser, F., Reitner, J.M., Radtke, U., 2007. Luminescence dating of proglacial sediments from the Eastern Alps. Quaternary International 164/165, 21–32.
Keller, B., 1996. Lithofazies-Codes für die Klassifikation von Lockergesteinen. Mitteilungen der Schweizerischen Gesellschaft für Boden- und Felsmechanik 132, 5–12.
Keller, O., Krayss, E., 1998. Datenlage und Modell einer Rhein-Linth-Vorlandvergletscherung zwischen Eem-Interglazial und Hochwürm. Geo-ArcheoRhein 2, 21–138.
von Klebelsberg, R., 1935. Geologie von Tirol. Gebrüder Borntraeger, Berlin.
Körner, C., 2003. Alpine Plant Life. Springer, Heidelberg.
Kühl, N., Litt, T., Schölzel, C., Hense, A., 2007. Eemian and Early Weichselian temperature and precipitation variability in northern Germany. Quaternary Science Reviews 26, 3311–3317.
Krenmayr, H.G., 2000. Sedimentologie der letzt-intergalzialen bis Mittelwürm-zeitlichen Seesedimente bei Mondsee. In: van Husen, D. (Ed.), Klimaentwicklung im Riss/Würm Interglazial (Eem) und Frühwürm (Sauerstoffisotopenstufe 6-3) in den Ostalpen. Mitteilungen der Kommission für Quartärforschung der Österreichischen Akademie der Wissenschaften, vol. 12, pp. 13–37.
Krüger, J., Kjær, K.H., 1999. A data chart for field description and genetic interpretation of glacial diamicts and associated sediments – with examples from Greenland, Iceland, and Denmark. Boreas 28, 386–402.
Lang, A., Hatté, C., Rousseau, D.-D., Antoine, P., Fontugne, M., Zöller, L., Hambach, U., 2003. High-resolution chronologies for loess: comparing AMS ^{14}C and optical dating results. Quaternary Science Reviews 22, 953–959.
Link, A., Preusser, F., 2005. Hinweise auf eine Vergletscherung des Kemptner Beckens (Südwest-Bayern) im Mittleren Würm. Eiszeitalter und Gegenwart 55, 64–87.
Lowick, S., Trauerstein, M., Preusser, F., 2012. Testing the application of post IR-IRSL dating to fine grain waterlain sediments. Quaternary Geochronology 8, 33–40.
Lukas, S., Preusser, F., Anselmetti, F.S., Tinner, W., 2012. Testing the potential of luminescence dating of high-alpine lake sediments. Quaternary Geochronology 8, 23–32.
Magny, M., 2007. Lake level studies/West-Central Europe. In: Elias, S.A. (Ed.), Encyclopedia of Quaternary Science. Elsevier, Amsterdam, pp. 1389–1399.

Meyer, M., Spötl, C., Mangini, A., 2008. The demise of the Last Interglacial recorded in isotopically dated speleothems from the Alps. Quaternary Science Reviews 27, 476–496.
Müller, U.C., 2000. A Late-Pleistocene pollen sequence from the Jammertal, southwestern Germany with particular reference to location and altitude as a factor determining Eemian forerst composition. Vegetation History and Archaeobotany 9, 125–131.
Müller, U.C., Pross, J., Bibus, E., 2003. Vegetation response to rapid climate change in Central Europe during the past 140,000 yr based on evidence from the Füramoos pollen record. Quaternary Research 59, 235–245.
Müller, U.C., Sánchez Goñi, M.F., 2007. Vegetation dynamics in southern Germany during Marine Isotope Stage 5 (~130 to 70 kyr ago). In: Sirocko, F., Claussen, M., Sánchez Goñi, M.F., Litt, T. (Eds.), The Climate of Past Interglacials. Developments in Quaternary Science, vol. 7. Elsevier, Amsterdam, pp. 277–287.
Nicolussi, K., Kaufmann, M., Patzelt, G., van der Plicht, J., Thurner, A., 2005. Holocene tree-line variability in the Kauner Valley, central Eastern Alps, indicated by dendrochronological analysis of living trees and subfossil logs. Vegetation History and Archaeobotany 14, 221–234.
North Greenland Ice Core Project (NGRIP) Members, 2004. High-resolution record of Northern Hemisphere climate extending into the last interglacial period. Nature 431, 147–151.
Ortner, H., Stingl, H., 2001. Facies and basin development of the Oligocene in the Lower Inn Valley, Tyrol/Bavaria. In: Piller, W., Rasser, M.W. (Eds.), Paleogene of the Eastern Alps. Schriftenreihe der Erdwissenschaftlichen Kommission der Österreichischen Akademie der Wissenschaften, vol. 14, pp. 153–196.
Penck, A., Brückner, E., 1909. Die Alpen im Eiszeitalter. Tauchnitz, Leipzig.
Pini, R., Ravazzi, C., Donegana, M., 2009. Pollen stratigraphy, vegetation and climate history of the last 215 ka in the Azzano Decimo core (plain of Friuli, northeastern Italy). Quaternary Science Reviews 28, 1268–1290.
Poscher, G., Eder, S., Marschallinger, R., Sedlacek, C., 2008. Trassenstudien in östlichen Inntalabschnitt. Felsbau Magazin 2, 92–102.
Prescott, J.R., Stephan, L.G., 1982. The contribution of cosmic radiation to the environmental dose for thermoluminescence dating – latitude, altitude and depth dependences. PACT 6, 17–25.
Preusser, F., 1999. Luminescence dating of fluvial sediments and overbank deposits from Gossau, Switzerland: fine grain dating. Quaternary Geochronology (Quaternary Science Reviews) 18, 217–222.
Preusser, F., 2003. IRSL dating of K-rich feldspars using the SAR protocol: comparison with independent age control. Ancient TL 21, 17–23.
Preusser, F., 2004. Towards a chronology of the Late Pleistocene in the northern Alpine Foreland. Boreas 33, 195–210.
Preusser, F., Kasper, H.U., 2001. Comparison of dose rate determination using high-resolution gamma spectrometry and inductively coupled plasma-mass spectrometry. Ancient TL 19, 19–23.
Preusser, F., Geyh, M.A., Schlüchter, C., 2003. Timing of Late Pleistocene climate change in lowland Switzerland. Quaternary Science Reviews 22, 1435–1445.
Preusser, F., Schlüchter, C., 2004. Dates from an important early Late Pleistocene ice advance in the Aare Valley, Switzerland. Eclogae Geologicae Helvetiae 97, 245–253.
Preusser, F., Degering, D., 2007. Luminescence dating of the Niederweningen mammoth site, Switzerland. Quaternary International, 164–165.
Preusser, F., Blei, A., Graf, H.R., Schlüchter, C., 2007. Luminescence dating of proglacial sediments from Switzerland. Boreas 36, 130–142.
Preusser, F., Fiebig, M., 2009. European Middle Pleistocene loess chronostratigraphy: some considerations based on evidence from the Wels site, Austria. Quaternary International 198, 37–45.
Preusser, F., Reitner, J.M., Schlüchter, C., 2010. Distribution, geometry, age and origin of overdeepened valleys and basins in the Alps and their foreland. Swiss Journal of Geosciences 103, 407–426.
Reitner, J.M., 2005. Quartärgeologie und Landschaftsentwicklung im Raum Kitzbühel – St. Johann i. T. – Hopfgarten (Nordtirol) vom Riss bis in das Würm-Spätglazial (MIS 6-2). PhD thesis University of Vienna, Austria.
Reitner, J.M., Gruber, W., Römer, A., Morawetz, R., 2010. Alpine overdeepenings and paleo-ice flow changes: an integrated geophysical-sedimentological case study from Tyrol (Austria). Swiss Journal of Geosciences 103, 385–405.
Rees-Jones, J., 1995. Optical dating of young sediments using fine-grain quartz. Ancient TL 13, 9–14.
Reimer, P.J., Baillie, M.G.L., Bard, E., Bayliss, A., Beck, J.W., Blackwell, P.G., Ramsey, C.B., Buck, C.E., Burr, G.S., Edwards, R.L., Friedrich, M., Grootes, P.M., Guilderson, T.P., Hajdas, I., Heaton, T.J., Hogg, A.G., Hughen, K.A., Kaiser, K.F., Kromer, B., McCormac, F.G., Manning, S.W., Reimer, R.W., Richards, D.A., Southon, J.R., Talamo, S., Turney, C.S.M., van der Plicht, J., Weyhenmeyer, C.E., 2009. IntCal09 and Marine09 radiocarbon age calibration curves, 0–50,000 years cal BP. Radiocarbon 51, 1111–1150.
Rousseau, D.-D., Derbyshire, E., Antoine, P., Hatté, C., 2007. Loess Records/Europe. In: Elias, S.A. (Ed.), Encyclopedia of Quaternary Science. Elsevier Amsterdam, pp. 1440–1456.
Sánchez Goñi, M.F., Loutre, M.F., Crucifix, M., Peyron, O., Santos, L., Duprat, J., Malaizé,, B., Turon, J.-L., Peypouquet, J.-P., 2005. Increasing vegetation and climate gradient in Western Europe over the Last Glacial Inception (122–110 ka): data-model comparison. Earth and Planetary Science Letters 231, 111–130.
Scheuer, C., 1996. Neuere Funde von *Arthrinium*-Arten (Hyphomycetes, Fungi imperfecti) aus Österreich. Österreichische Zeitschrift für Pilzkunde 5, 1–21.
Schlüchter, C., 1991. Fazies und Chronologie des letzteiszeitlichen Eisaufbaues im Alpenvorland der Schweiz. In: Frenzel, B. (Ed.), Klimageschichtliche Probleme der letzten 130000 Jahre. G. Fischer Stuttgart, New York, pp. 401–407.
Schlüchter, C., 2004. The Swiss glacial record: a schematic summary. In: Ehlers, J., Gibbard, P.L. (Eds.), Quaternary Glaciations: Extent and Chronology Part I: Europe. Elsevier, London, pp. 413–418.
Schlüchter, C., Maisch, M., Suter, J., Fitze, P., Keller, W.A., Burga, C.A., Wynistorf, E., 1987. Das Schieferkohlenprofil von Gossau Kanton Zürich und seine stratigraphische Stellung innerhalb der letzten Eiszeit. Vierteljahresschrift der Schweizerischen Naturforschenden Gesellschaft Zürich 132, 135–174.
Sperazza, M., Moore, J.N., Hendrix, M.S., 2004. High-resolution particle size analysis of naturally occurring very fine-grained sediment through laser diffractometry. Journal of Sedimentary Research 74, 736–743.
Spötl, S., Mangini, A., 2002. Stalagmite from the Austrian Alps reveals Dansgaard–Oeschger events during isotope stage 3: Implications for the absolute chronology of Greenland ice cores. Earth and Planetary Science Letters 203, 507–518.
Spötl, C., Mangini, A., Richards, D.A., 2006. Chronology and paleoenvironment of Marine Isotope Stage 3 from two high-elevation speleothems, Austrian Alps. Quaternary Science Reviews 25, 1127–1136.
Spötl, C., Mangini, A., 2006. U/Th age constraints on the absence of ice in the central Inn Valley (Eastern Alps, Austria) during Marine Isotope Stages 5c to 5a. Quaternary Research 66, 167–175.
Spötl, C., Holzkämper, S., Mangini, A., 2007. The Last and the Penultimate Interglacial as recorded by speleothems from a climatically sensitive high-elevation cave site in the Alps. In: Sirocko, F., Claussen, M., Sánchez Goñi, M.F., Litt, T. (Eds.), The Climate of Past Interglacials. Developments in Quaternary Science, vol. 7. Elsevier, Amsterdam, pp. 471–491.
Starnberger, R., Rodnight, H., Spötl, C. Luminescence dating of fine-grain lacustrine sediments from the Eastern Alps-examples from Unterangerberg (Austria). Austrian Journal of Earth Sciences, submitted for publication.
Stockmarr, J., 1971. Tablets with spores used in absolute pollen analysis. Pollen et Spores 13, 615–621.
Stuiver, M., Polach, H.A., 1977. Reporting of ^{14}C data – discussion. Radiocarbon 19, 355–363.
Stuiver, M., Reimer, P.J., Reimer, R.W., 2005. CALIB 6.0 (WWW program and documentation). http://calib.qub.ac.uk/calib/.
Svensson, A., Andersen, K.K., Bigler, M., Clausen, H.B., Dahl-Jensen, D., Davies, S.M., Johnsen, S.J., Muscheler, R., Parrenin, F., Rasmussen, S.O., Röthlisberger, R., Seierstad, I., Steffensen, J.P., Vinther, B.M., 2008. A 60 000 year Greenland stratigraphic ice core chronology. Climate of the Past 4, 47–57.
Thiel, C., Buylaert, J.-P., Murray, A.S., Terhorst, B., Hofer, I., Tsukamoto, S., Frechen, M., 2010. Luminescence dating of the Stratzing loess profile (Austria) – testing the potential of an elevated temperature post-IR IRSL protocol. Quaternary International 234, 23–31.
Thiel, C., Buylaert, J.-P., Murray, A.S., Terhorst, B., Tsukamoto, S., Frechen, M., Sprafke, T., 2011. Investigating the chronostratigraphy of prominent paleosols in Lower Austria using post-IR IRSL dating. Quaternary Science Journal 60, 137–152.
Thomsen, K., Murray, A.S., Jain, M., Bøtter-Jensen, L., 2008. Laboratory fading rates of various luminescence signals from feldspar-rich sediment extracts. Radiation Measurements 43, 1474–1486.
Tucker, M., 2003. Sedimentary Rocks in the Field. John Wiley & Sons, Chichester.
Tzedakis, P.C., 2005. Towards an understanding of the response of southern European vegetation to orbital and suborbital climate variability. Quaternary Science Reviews 24, 1585–1599.
Vandenberghe, J., Lowe, J., Coope, R., Litt, T., Zöller, L., 2004. Climatic and environmental variability in the mid-latitude Europe sector during the last Interglacial–Glacial cycle. In: Battarbee, R.W. (Ed.), Past Climate Variability through Europe and Africa. Springer, Dordrecht, pp. 393–416.
Van Geel, B., 1978. A palaeoecological study of Holocene peat bog sections in Germany and the Netherlands, based on the analysis of pollen, spores, fungi, algae, cormophytes and animals. Review of Palaeobotany and Palynology 25, 1–120.
Van Geel, B., Bohncke, S.J.P., Dee, H., 1981. A palaeoecological study of an upper late glacial and Holocene sequence from "The Borchert", The Netherlands. Review of Palaeobotany and Palynology 31, 367–448.
Van Geel, B., Hallewas, D.P., Pals, J.P., 1983. A Late Holocene deposit under the Westfriese Zeedijk near Enkhuizen (Prov. of N-Holland, The Netherlands): palaeoecological and archaeological aspects. Review of Palaeobotany and Palynology 38, 269–335.
Van Geel, B., Coope, G.R., van der Hammen, T., 1989. Palaeoecology and stratigraphy of the Late-glacial type section at Usselo (The Netherlands). Review of Palaeobotany and Palynology 60, 25–129.
Van Meerbeeck, C.J., Renssen, H., Roche, D.M., Wolfarth, B., Bohncke, S.J.P., Bos, J.A.A., Engels, S., Helmens, K.F., Sánchez-Goñi, M.F., Svensson, A., Vandenberghe, J., 2011. The nature of MIS 3 stadial-interstadial transitions in Europe: New insights from model-data comparison. Quaternary Science Reviews 30, 3618–3637.
Wallinga, J., Murray, A., Wintle, A., 2000. The single-aliquot regenerative-dose (SAR) protocol applied to coarse-grain feldspar. Radiation Measurements 32, 529–533.
Welten, M., 1982. Pollenanalytische Untersuchungen im jüngeren Quartär des nördlichen Alpenvorlandes der Schweiz. Beiträge zur Geologischen Karte der Schweiz 156, 1–174.

Wick, L., 2006. Full- to late-glacial vegetation and climate changes and evidence of glacial refugia in the south-eastern Alps (Italy). XXX International Moor-Excursion 2006, Northern and Central Italy, 16.9–24.9.2006. Excursion Guide, 53–55.

Wintle, A.G., Murray, A.S., 2006. A review of quartz optically stimulated luminescence characteristics and their relevance in single-aliquot regeneration dating protocols. Radiation Measurements 41, 369–391.

Wolff, E.W., Chappellaz, J., Blunier, T., Rasmussen, S.O., Svensson, A., 2010. Millennial-scale variability during the last glacial: The ice core record. Quaternary Science Reviews 29, 2828–2838.

Zöller, L., Oches, E.A., McCoy, W.D., 1994. Towards a revised chronostratigraphy of loess in Austria with respect to key sections in the Czech Republic and in Hungary. Quaternary Geochronology (Quaternary Science Reviews) 13, 465–472.